Opto-Electronic Science

Review

2022, Vol. 1, No. 9

DOI: 10.29026/oes.2022.220010

All-optical logic gate computing for high-speed parallel information processing

Shuming Jiao[1]*, Junwei Liu[2]*, Liwen Zhang[1], Feihong Yu[3], Guomeng Zuo[1,3], Jingming Zhang[3], Fang Zhao[3], Weihao Lin[3] and Liyang Shao[1,3]*

Optical computing and optical neural network have gained increasing attention in recent years because of their potential advantages of parallel processing at the speed of light and low power consumption by comparison with electronic computing. The optical implementation of the fundamental building blocks of a digital computer, i.e. logic gates, has been investigated extensively in the past few decades. Optical logic gate computing is an alternative approach to various analogue optical computing architectures. In this paper, the latest development of optical logic gate computing with different kinds of implementations is reviewed. Firstly, the basic concepts of analogue and digital computing with logic gates in the electronic and optical domains are introduced. And then a comprehensive summary of various optical logic gate schemes including spatial encoding of light field, semiconductor optical amplifiers (SOA), highly nonlinear fiber (HNLF), microscale and nanoscale waveguides, and photonic crystal structures is presented. To conclude, the formidable challenges in developing practical all-optical logic gates are analyzed and the prospects of the future are discussed.

Keywords: logic gate; optical computing; artificial intelligence; waveguide; crystal structure

Jiao SM, Liu JW, Zhang LW, Yu FH, Zuo GM et al. All-optical logic gate computing for high-speed parallel information processing. *Opto-Electron Sci* **1**, 220010 (2022).

Introduction

Nowadays the global demand for computing is ever-increasing and the development of electronic computers faces bottlenecks of power consumption, heat dissipation and response speed. Compared with electronic computing, optical computing has the potential advantages of high-speed parallel processing and low power consumption.

Computer technology can be divided into two categories: analog computing and digital computing. In the realm of digital computing, logic gates are indispensable devices and have been investigated extensively. An analogue computer models a computational task using continuously varying quantities of physical phenomena. Digital computing uses binary encoding to process discrete quantities. For electronic computers, digital computing is the dominant architecture because it has considerably better accuracy, reliability and flexibility than analogue computing. It is still debatable whether the mainstream architecture of future optical computing will be analogue or digital. Both all-optical analogue computing[1–17] and all-optical digital computing[18–22] have been investigated extensively in the past few decades. All-optical digital computing is at least one of the feasible approaches to achieve the final objective of all-optical computing and artificial intelligence. In addition, a huge amount of data is transmitted worldwide through optical fibers every day and optical signal processing of transmitted data[23–25] is

[1]Peng Cheng Laboratory, Shenzhen 518055, China; [2]Department of Physics, The Hong Kong University of Science and Technology, Hong Kong 999077, China; [3]Department of Electrical and Electronic Engineering, Southern University of Science and Technology, Shenzhen 518055, China.
*Correspondence: SM Jiao, E-mail: jiaoshm@pcl.ac.cn; JW Liu, E-mail: liuj@ust.hk; LY Shao, E-mail: shaoly@sustech.edu.cn

Received: 25 May 2022; Accepted: 27 June 2022; Published online: 7 September 2022

another crucial application for all-optical logic gates. All-optical signal processing of transmitted data includes encoding, decoding, format conversion, encryption, switching, routing, multiplexing, error correction, etc.

In a modern digital computing system, logic gates are the fundamental building blocks. Sophisticated computation tasks (e.g. a deep learning neural network with complicated structures) can ultimately be decomposed into basic logic gate operations. A logic gate can execute a Boolean function, normally with two binary input values and one binary output value. There are different types of logic gates (e.g. NOT, AND, OR, XOR, NAND, NOR, XNOR) with varying input-output rules, as shown in Table 1. Individual logic gates can be interconnected to create a logical circuit to perform more complex calculations. A number of NOR or alternatively NAND gates can be used to reproduce the function of all other logic gates. Both NOR and NAND gates are referred to as universal gates. Even though some effort has been made to customize a new set of optical logic rules[26,27], the Boolean logic rules are still widely adopted by most works in the field of optical computing.

Logic gates can be realized easily by transistors in an electronic computer. A transistor is a kind of switch in which the binary state of one electronic signal is controlled by another electronic signal. However, there is no optical device exactly analogous to an electronic transistor. The optical implementation of logic gates is a very challenging technology and has received extensive attention in recent decades. A timeline of advances in optical logic gates and related technologies is shown in Fig. 1. The basic idea is to use one light signal to control the

Table 1 | Truth tables of common logic gates (A and B are input binary values; X is logic gate output).

NOT — $\overline{A}$

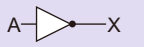

A	X
0	1
1	0

AND — AB

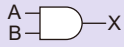

A	B	X
0	0	0
0	1	0
1	0	0
1	1	1

NAND — $\overline{AB}$

A	B	X
0	0	1
0	1	1
1	0	1
1	1	0

OR — $A+B$

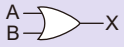

A	B	X
0	0	0
0	1	1
1	0	1
1	1	1

NOR — $\overline{A+B}$

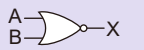

A	B	X
0	0	1
0	1	0
1	0	0
1	1	0

XOR — $A \oplus B$

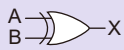

A	B	X
0	0	0
0	1	1
1	0	1
1	1	0

XNOR — $\overline{A \oplus B}$

A	B	X
0	0	1
0	1	0
1	0	0
1	1	1

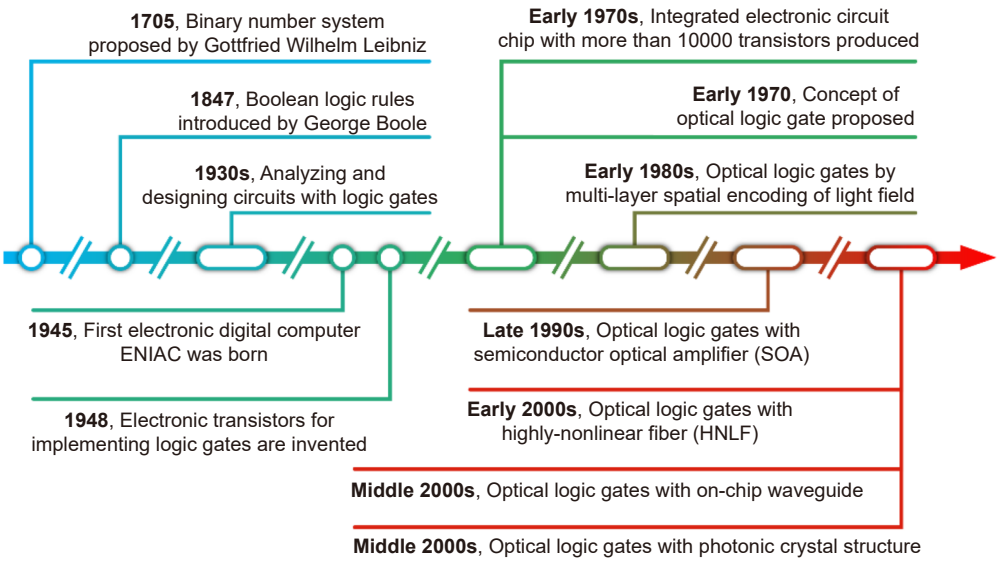

Fig. 1 | Timeline of advances in optical logic gates and related technologies.

binary state of another light signal. The number of logic gate operations per second for an electronic transistor is usually limited within an upper bound by its physical working mechanism. Optical signals can theoretically be processed at a much higher frequency than an electronic transistor. Therefore, ideally, the response time of optical logic gate is very short. Hence, many different schemes for optical logic gate have been proposed. There is no doubt that depending upon the scenarios for which the optical logic gates are applied, the possibilities for the future are endless. At present, optical logic gates are implemented in a wide variety of ways. In this paper, five types of optical logic gates are mainly introduced, spatial encoding of light fields, semiconductor optical amplifiers (SOA), highly-nonlinear fiber (HNLF), microscale and nanoscale waveguides, and photonic crystal structures, as shown in Fig. 2. By comparison with previous literature reviews of all-optical logic gate computing[18–22], this is a more comprehensive summary that includes several optical technologies not covered previously and many recent studies in the past three years. The working principles of different optical logic gate schemes are described in the following sections.

Spatial encoding of light field

Spatial encoding of the light field is a simple and straightforward way of performing optical logic gate operations. When the light field is spatially encoded with respect to its distribution of intensity, phase, polarization or other dimensions, it can carry a certain amount of binary information. If the light propagates and interacts with a properly encoded mask, this binary information can be transformed according to the rules of binary logic operations. As a simple example of light-intensity spatial encoding, a thin film can be divided into many small cells and each cell can be either transparent or opaque, representing the binary states "1" and "0" respectively. When corresponding cells of two thin films overlap under conventional illumination, the light will be blocked if either cell is opaque, resulting in a dark state (binary state "0"). This is equivalent to the AND logic

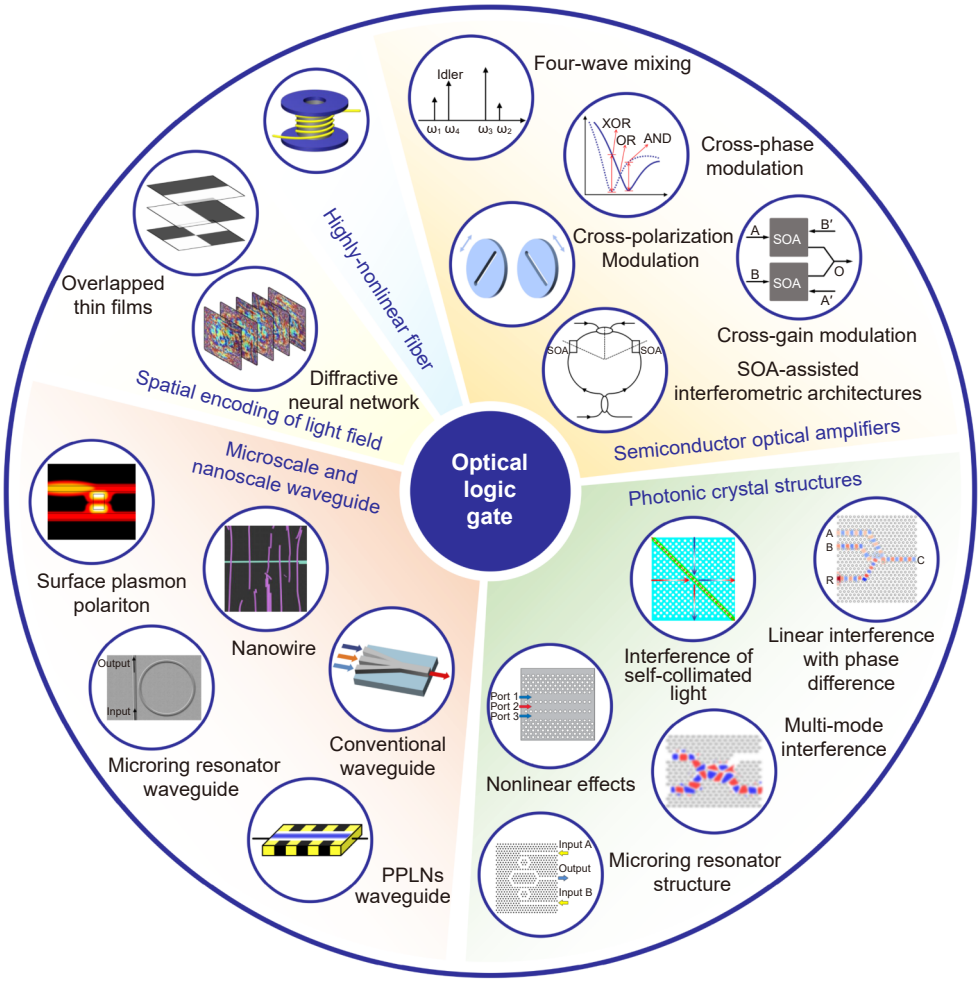

Fig. 2 | Overview of various optical logic gate schemes.

operation. In fact, all sixteen binary gate operations can be realized by overlapping multiple transparency-encoded thin films with or without spatially encoded light illumination patterns[28–32]. A representative scheme is described in ref.[30].

For inputs A and B, the four combinations of binary values are represented by a cell consisting of four sub-cells. Only one of the four sub-cells will be white (transparent) and the remaining three are black (opaque) as shown in Fig. 3(a). Then the input cell denoting A & B and a particular gate cell are aligned and overlapped. Each gate cell is also composed of four sub-cells and different gate cells are encoded according to the truth table, as shown in Fig. 3(b). Finally, in the overlapping result, a cell is "0" if all the sub-cells are black and "1" if any sub-cell is white regardless of its position. This optical logic gate scheme is similar to the visual cryptography concept[33–35], where multiple layers of thin films are overlapped for image pattern hiding.

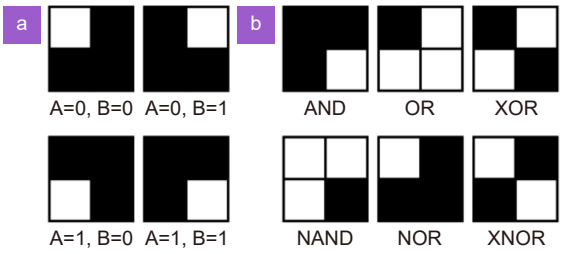

Fig. 3 | Optical logic gates created by the superposition of spatially encoded transparent thin films: (**a**) cells encoded for binary input; (**b**) cells encoded for different logical operations[30].

In addition to transparency, the polarization state of each cell in a mask can be also encoded for optical logic computing[36,37]. For example, if one cell is encoded as vertically polarized, a light with horizontal polarization direction will be blocked. However, controlling the output light intensity by modulating the polarization of light can be suboptimal. A direct representation of binary bit values with the same light intensity and two orthogonal polarization states is preferable[38–42]. The interaction between polarized light and a number of polarization modulation masks are used to implement logic gates[40–42]. One polarized optical input and one electronic input controlling the mask can jointly be converted to a polarized optical logic gate output.

In a recent work[43], a diffractive neural network system has been employed to perform optical logic gate operations, shown in Fig. 4. An input coherent plane light wave is spatially encoded with respect to the intensity distribution according to two input binary values and the type of logic gate operation. Then, the light field propagates forward and is modulated sequentially by several metasurface phase masks placed separately by a certain distance. All the phase mask pixels are optimally encoded. Finally, the light field is focused by the free-space diffraction and phase mask modulation onto one of the two target regions, representing logical outputs "1" and "0" respectively. A recent work shows that the multiple-layer system can be simplified to a single-layer metasurface[44]. Alternatively, the logic states can be represented by linear momentums instead of intensity distributions in a diffractive neural network system[45].

Some spatial encoding methods for binary optical logic operations only need very simple and low-cost optical setups, such as two overlapping thin films. The proposed systems can potentially perform binary logic operations in parallel for many input bits simultaneously. However, they generally have the limitation that the input and output binary values are represented in an encoded format. Interconnecting a previous gate's output to the next gate's input can be a challenge[46]. Since some non-optical encoding and decoding steps may be required

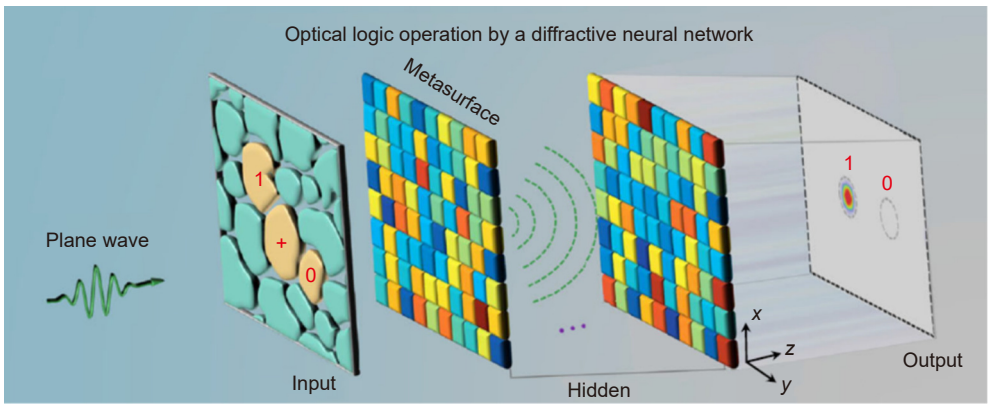

Fig. 4 | Performing logic gate operations optically with a diffractive neural network system. Figure reproduced from ref.[43], under a Creative Commons Attribution 4.0 International License.

if multiple logic gate operations are cascaded, it is difficult to construct an efficient large-scale fully optical logic gate circuit.

Semiconductor optical amplifiers (SOA)

An SOA is a compact semiconductor device that can be controlled to amplify a light signal. There are several nonlinear effects in SOA, including cross-gain modulation, cross-phase modulation, four-wave mixing and cross-polarization modulation, which can be exploited to design logic gates[47,48]. SOAs can either operate logic functions alone or in collaboration with interferometric architectures.

Cross-gain modulation (XGM)

XGM has been investigated extensively to design optical logic gates with SOA[49–53]. It is assumed that there are two input light beams for each SOA. One is the probe light and the other is the much stronger pump light. The probe light cannot pass through the SOA when the pump light saturates it. The probe light can go through the SOA when the pump light is absent. There is an inverse relationship between the intensity of the output probe light and pump light, referred to as the XGM effect. An XOR gate can be realized using two SOAs based on the XGM effect[54], as shown in Fig. 5(a).

In this system, two input light signals A and B are simultaneously transmitted to two SOAs for corresponding optical signal amplification. The output signals of the two SOAs are combined. When both A and B are 0, the output will be certainly 0 since there is no input probe signal. When A and B are both 1, the output will be still 0 since both two SOAs block the pass of probe signals. However, when A=0, B=1 or A=1, B=0, the probe signal will pass one of the SOAs and the output signal is 1. These results are consistent with the XOR logic gate rules.

Other logic gates such as NOR, AND, NAND and AND –NOR can be implemented with different SOA configurations using XGM as well[49–52]. For example, if one probe signal in Fig. 5(a) is replaced with a clock signal with constant non-zero intensity shown in Fig. 5(b), a NAND gate can be realized[51]. The system will only have a zero output when both A and B are 1.

Cross-phase modulation (XPM)

The pump light injected into a SOA will modulate not only the amplitude but also the phase of probe light. The XPM is more commonly combined with interferometric architectures to implement optical logic gates. However, a transient cross-phase modulation (T-XPM) with picosecond-pulse injection can be employed to implement various logic gates using a single SOA and band pass filters[55,56], shown in Fig. 6.

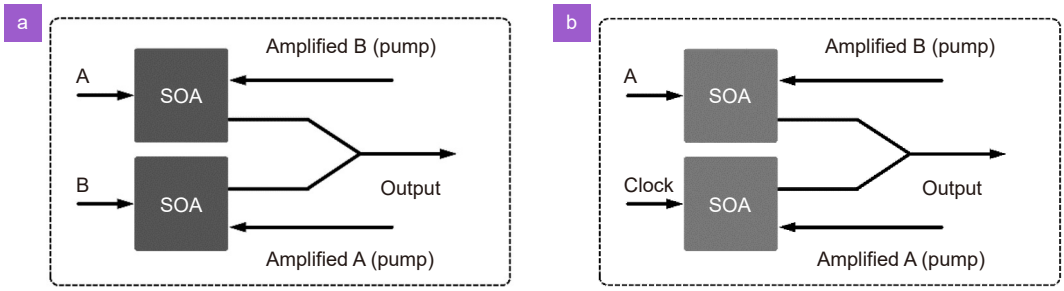

Fig. 5 | (**a**) XOR gate with two SOAs based on XGM effect (input A and B). (**b**) NAND gate with two SOAs based on XGM effect (input A and B).

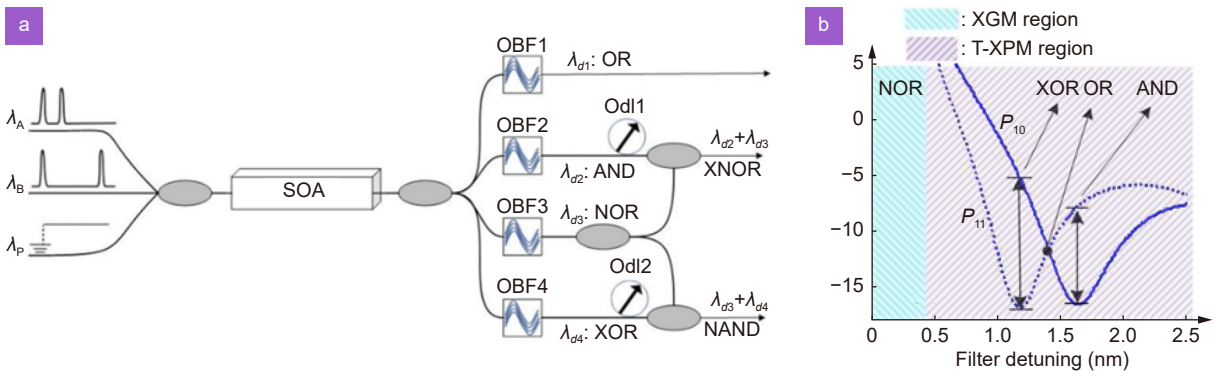

Fig. 6 | Optical logic gates with SOA based on T-XPM: (**a**) optical setup; (**b**) frequency spectrum of the output probe signal. Figure reproduced with permission from ref.[56], © The Optical Society.

Two input signals A and B are both used as the pump light and there is an additional probe light signal. Because of XPM, the output probe signal will have different frequency spectra when the two input signals are both 1 (P_{11}) or only one input signal is 1 (P_{10}). By performing bandpass filtering at the selected frequency, various logic gates can be implemented and the filtered light intensity is taken as the output of the logic gate.

Four-wave mixing (FWM)

As shown in Fig. 7, FWM occurs when three input signals ω_1, ω_2 and ω_3 with different frequencies, or two input signals ω_1 and ω_2 with different frequencies, are transmitted to SOA. The latter case is referred to as degenerate FWM. In FWM, a new idle signal with a different frequency ω_4 $(\omega_4 = \omega_1 + \omega_2 - \omega_3)$ will be yielded. If the original phases of the three input signals are φ_1, φ_2 and φ_3 respectively, the phase of the idle signal will be φ_4 $(\varphi_4 = \varphi_1 + \varphi_2 - \varphi_3)$. For the degenerate case, the idle signal will have a frequency of ω_3 $(\omega_3 = 2\omega_1 - \omega_2)$ and a phase of φ_3 $(\varphi_3 = 2\varphi_1 - \varphi_2)$.

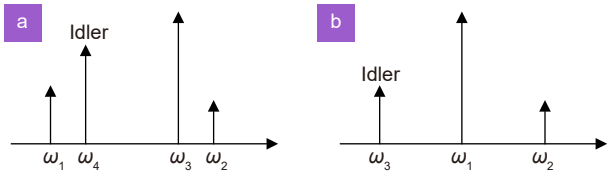

Fig. 7 | (**a**) Four-wave mixing. (**b**) Degenerate four-wave mixing.

For degenerate FWM, the idle signal can only be generated when two input signals at ω_1 and ω_2 are both present, which can be considered as an inherent AND gate[57]. Alternatively, when one input signal ω_1 is constantly non-zero and one of the other two signals ω_2 and ω_3 is non-zero or both are non-zero, the same idle signal can be generated if $2\omega_1 - \omega_2 = 2\omega_3 - \omega_1$. This is equivalent to an OR operation[58].

In addition, it should be noted that FWM only occurs when the polarization states of all the input signals are identical. The idle signal generated will also have the same polarization state. Logic gate computing with degenerate FWM can be implemented using this property[59]. For example, two input signals are encoded as being in one of two orthogonal polarization directions r or s representing binary input values 0 or 1 respectively. When both input signals have identical polarization states, the intensity of the output idler signal will be non-zero (representing 1). Otherwise, the idler signal will not be generated and has zero intensity (representing 0). Thus, an XNOR gate is obtained. Further, by only detecting the intensity of the idler signal in only one polarization direction, a logic value 1 is only obtained when both input signals are 0 (r state) or both input signals are 1 (s state). Consequently, NOR and AND gates can be realized.

An alternative approach of designing logic gates is based on the phase relationship[60–63]. The binary logic values 0 and 1 are represented by the phase 0 and π of input (or output) signal respectively. The input signals at ω_1 and ω_2 carry data and the input signal at ω_3 has a constant phase. The constant phase can become 0 after cancellation. Therefore the phase of idle signal is $\varphi_4 = \varphi_1 + \varphi_2$. If $\varphi_1 = \pi$, $\varphi_2 = \pi$, and $\varphi_4 = 2\pi$ (equivalent to 0), an XOR gate operation can be performed base on this relationship.

When FWM is combined with other effects such as XGM and T-XPM, a multi-function reconfigurable system for multiple types of logic gates can be constructed[64–68].

Cross-polarization modulation (CPM)

The CPM in an SOA can modify the polarization state of the input signal and has been investigated for implementing different logic gates such as XOR, AND, OR and NAND[69–73]. As an example, we use the implementation of an AND gate[72] to illustrate the working principle of CPM, as shown in Fig. 8. A pump signal and a probe signal at two different frequencies are injected into the SOA. A polarizer is placed in the output of the SOA. Originally, the polarization direction of the probe signal is orthogonal to that of the polarizer. If the probe signal alone is 1, the final orthogonally polarized output signal passing through the polarizer will also be 0. If the input probe signal is 0, regardless of the pump signal intensity, it is evident that the final probe output will be 0. When both the probe signal and pump signal are present, the pump signal changes the polarization state of the probe signal because of CPM. Then the polarization directions of the probe signal and polarizer will be only partially orthogonal and some amount of the probe signal will pass through the polarizer. In consequence, the output probe signal will only be 1 under this circumstance resulting in an AND gate.

SOA-assisted interferometric architectures

The XPM effect in SOA can impose a phase shift on the input light signal and the phase change can be converted

to a more easily detectable intensity change by interference. Consequently, SOA-assisted interferometric architectures have been explored extensively. SOA is most commonly combined with Mach–Zehnder interferometer (MZI) and Sagnac interferometer[74].

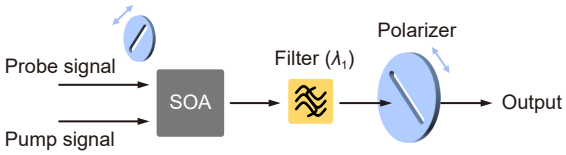

Fig. 8 | Optical AND logic gates with SOA based on CPM.

SOA-MZI configuration

In the SOA-MZI configuration, two SOAs are usually placed in the upper and lower arms respectively. Copropagation[75–85] and counterpropagation[86–88] are two typical configurations of SOA-assisted MZI, as shown in Fig. 9. The operating principles of these two configurations are similar. Two data signals A and B are each launched into one of the two arms, correspondingly. A probe signal (clock pulse) is split equally into two arms and recombined at the T-port through two 3 dB couplers (1∶1 couplers) in the MZI. From the working mechanism of MZI, the output probe signal from the upper arm and that from the lower arm will have a π phase difference if both data signals are 0. There will be destructive interference and the output probe signal will be also 0. On the other hand, if both the data signals are 1, the phase of probe signal in each arm will be modified in the same way by XPM in SOA. In the T-port, the final output will still be 0 since the relative phase difference is still π. However, if only the data signal for the upper arm or the lower arm is 1 (the other is 0), the probe signals in the two arms will have an extra phase difference and destructive interference will not occur at the T-port. In this condition, the output probe signal in the T-port will be 1. Consequently, the SOA-MZI configuration can be employed to construct an XOR gate[75–78,86–87]. One advantage of the counterpropagation configuration over the copropagation configuraton is that the filters in the output do not need to reject control signals as they propagate inversely[87].

Other logic gates such as AND and NAND gates can be realized by a slightly modified SOA-MZI system[79–81,88]. For example, an AND gate can be realized by removing the data signal in the lower arm or adding an extra probe signal in the upper arm[79,80]. When two or more SOA-MZI configurations are combined in parallel, more diverse logic gates can be implemented[82–85] including NOR, OR, XNOR and NAND gates.

Sagnac interferometer configuration

The Sagnac interferometer, referred to as a terahertz optical asymmetric demultiplexer (TOAD)[89] in some studies, consists of a loop with clockwise and counter-clockwise propagating light signals. SOAs can be placed at appropriate positions in the loop to implement logic gate operations[90–95]. An example of an XOR gate configuration with two symmetric SOAs is shown in Fig. 10(a). The probe signal is split equally by a 3 dB coupler and two separate light signals propagate clockwise and counter-clockwise. When both data signals are 0 and the two SOAs are off, two counterpropagating probe signals finally recombine with phase difference π at the output Port D. This destructive interference will yield an output probe signal of 0. When both data signals are 1 , the two symmetric SOAs will impose an identical XPM effect on

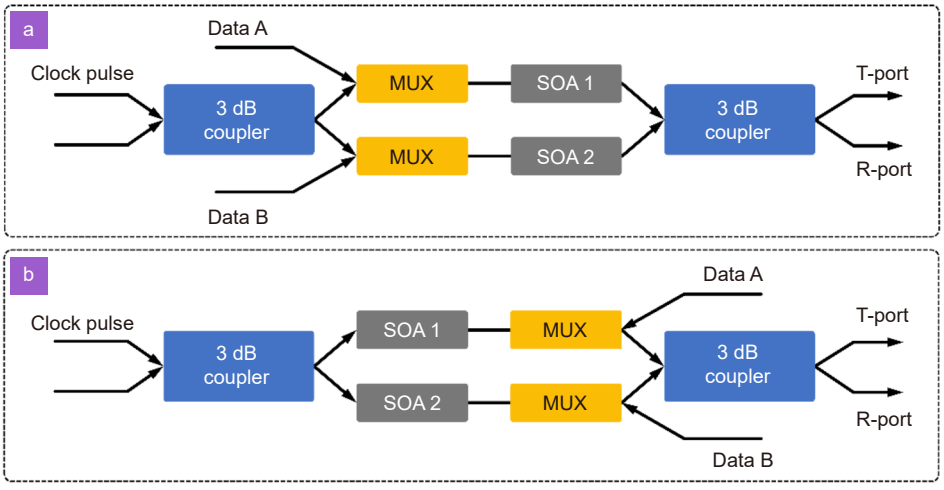

Fig. 9 | SOA-MZI configuration: (**a**) copropagation; (**b**) counterpropagation.

both clockwise propagating signals and counter-clockwise propagating signals since data A only affects the right SOA and data B only affects the left SOA. The relative phase difference will still be π and the output will be 0. When only data A or data B is 1, constructive interference will occur and the output probe signal will be 1 . If only one data signal is used, then there will be an AND relationship between the data signal and probe signal, as shown in Fig. 10(b).

In this configuration, two SOAs[90,91,93] can be replaced with a single SOA[92,94]. When multiple SOA-assisted Sagnac interferometers are cascaded and combined, more logic functions can be realized[95].

Furthermore, SOA can be combined with other interferometric configurations including Michelson interferometers (MI)[43], ultrafast nonlinear interferometers (UNI)[96–98,49] and delayed interferometers (DI)[99–103]. Compared with the SOA architecture, SOA-assisted interferometer architecture is generally more suitable for integration but its stability is poor and it is affected by additional noise[20].

Despite the advantages mentioned above, SOA is relatively slow to take off because of the time it takes to recover gain and phase. A new type of SOA, Quantum dot SOA (QD-SOA) can achieve a much greater speed of operation[104–112]. Another two types of SOA, reflective SOAs (RSOA)[113] and photonic crystal SOAs[114], have also been attempted recently.

Highly-nonlinear fiber (HNLF)

When a light signal propagates through a HNLF, the refractive index of the fiber material will change due to the Kerr effect. Multiple light signals will interact with each other when they pass through a HNLF. Different nonlinearity effects like those in SOAs are also present in a HNLF including self-phase modulation (SPM), cross phase modulation (XPM), four wave mixing (FWM) and polarization rotation.

As with the T-XPM in SOA, SPM and TPM can broaden the spectrum of output light signals when input signals are injected into the HNLF. Various logic gates can be implemented using a band pass filter for a selected frequency band[115–117]. In a three-input system[116] as shown in Fig. 11(a), one probe signal and two data signals are launched into the HNLF. When both data signals are 0 (off), one of them is 1 (on) or both of them are 1 (on), the output probe signal has three different spectra as shown in Fig. 11(b). Certain critical frequencies correspond to different logic operations if the filtered output light signal intensity is used to indicate the output value of the logic gate.

The SPM and CPM of HNLF can be combined with an optical loop mirror interferometric architecture to implement logic gates[118,119]. The FWM effect of HNLF can be exploited to realize logic gates based on the idle signal strength[120], polarization relationship[121] and phase relationship[122,123]. The working principles are very similar to the corresponding SOA systems[58–68]. Like CPM in SOA, the polarization rotation property of HNLF can be used to perform an XOR operation[124].

An HNLF can usually support a much higher data rate than an SOA and the fiber nonlinearity has a femtosecond response time. However, HNLF typically has a length of several meters to several kilometers, presenting a challenging drawback in terms of fabrication and integration.

Microscale and nanoscale waveguide

A waveguide is a structure used to guide electromagnetic waves, including light. It can be fabricated with various

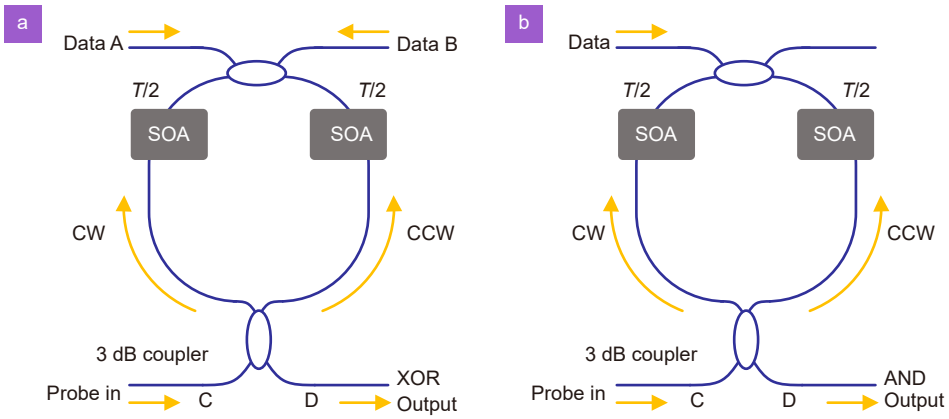

Fig. 10 | SOA assisted Sagnac configuration: (**a**) XOR gate[90]; (**b**) AND gate[93].

materials into diversified geometric forms. An on-chip optical waveguide consisting of a germanium (Ge)-doped silica core and an undoped silica cladding on top of a silicon substrate is widely used. Other common material platforms include but not limited to III-V semiconductor materials, lithium niobate, silicon nitride-on-insulator, and silicon-on-insulator. The common geometries include slab waveguide, ridge waveguide, rib waveguide, slot waveguide, and planar waveguide. Optical logic gates can be implemented by waveguide architectures using various nonlinear effects[125–134] and linear interference[135–143]. Waveguide devices can be ultracompact at microscale or even at nanoscale and driven by low power. It has great potential for integration with electronic devices.

General logic gate implementation with waveguide

The common nonlinearity effects in a waveguide include FWM[126–128], two-photon absorption (TPA)[130,131], free carrier effect[131,133], Raman scattering[132,133], XPM[133] and nonlinear slot-waveguide coupling[134].

The polarization relationship in FWM can be employed to implement various logic gates[126,127]. Only when both input signals are co-polarized and aligned to the TM (or TE) mode of the silicon waveguide, FWM will generate an idle output signal of a new frequency. Otherwise, FWM will not occur when the input signals have orthogonal polarization states. The phase relationship in FWM can also be used to implement an XOR gate with a planar waveguide. For example, a chalcogenide waveguide is a suitable candidate for this kind of operation[128,129].

A high power signal can deplete a low power signal in a silicon waveguide by TPA[130,131]. The data signals A and B with a low-power probe signal are injected into a waveguide together. When A and B are both equal to 0 and the total pump signal power is below the TPA threshold, the probe signal will not be absorbed and its output is 1. If there are only signals A or B, or if there are both signals A and B, the probe signal cannot pass through the waveguide due to TPA. This is a NOR gate operation based on TPA. It has been demonstrated that optical logic gates can be implemented in a silicon-on-insulator waveguide by using three nonlinear phenomena including stimulated Raman scattering, the free carrier effect, and XPM[133].

The light signals in two-slot silicon waveguides placed close to each other may be coupled under certain conditions[134]. By injecting quasi-TM mode and quasi-TE mode light waves into the input ports of two slot waveguides, the coupling can be enabled or disabled. The signal intensity at the output port of one slot waveguide can indicate the logic gate output. NOT, OR, and AND logic gates can be realized.

The linear interference of coherent light signals in a waveguide is also important in logic gate design[135–143]. It is well known that two light waves with phase difference 0 will interfere constructively (maximum intensity) and two light waves with phase difference π will interfere destructively (minimum intensity). The amplitude of each individual light wave will also affect the final result of interference. There are basically two ways to modulate the amplitude and phase of multiple input light signals to generate a desirable interference output to implement logic gates.

One approach is to optimize the length and loss of each waveguide path[136,142] as shown in Fig. 12. In Fig. 12(a), the path length from Input A port to the output port is identical to that of Input B port. For two identical coherent input light signals, the output signal will have

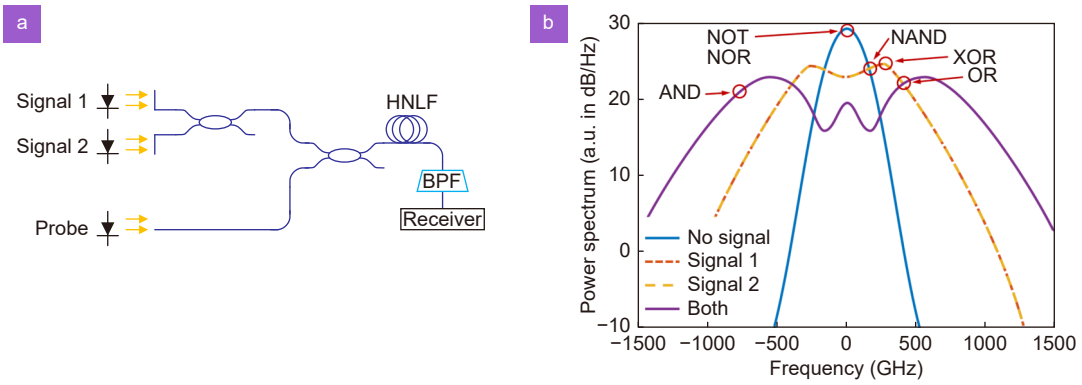

Fig. 11 | (**a**) Multi-function optical logic gate system based on HNLF. (**b**) Frequency spectrum of the output probe signal and logic gate design. Figure reproduced from ref.[116], IEEE.

enhanced intensity. An OR gate can be realized approximately. In Fig. 12(b), the path length from Input B port to the output port is $\lambda/2$ (λ denotes the wavelength) longer than that of Input A port, corresponding to a phase difference π. When only Input A or Input B is 0, the output will be 1. When both input signals are 1, the output will be 0 due to destructive interference. An XOR gate can thus be realized. In Fig. 12(c), the paths from C and B are $3\lambda/2$ and 2λ longer than that of A respectively, corresponding to phase differences π (3π) and 0 (4π). Hence the input signals from C and B will interfere destructively, the input signals from C and A will interfere destructively, but input signals from A and B will interfere constructively. The input signal from C is always present as a reference and the output will be 1 if both the signals from A and B are 0. When only the input signal from A or B is 1, the output will be 0 due to destructive interference. When the input signals from A and B are both 1, the signal will interfere constructively at first, and then the enhanced signal interferes destructively with the signal from C. However, the final output is still 1, since the enhanced combined signal has much higher intensity than the signal from C. An XNOR gate can be realized based on the working principles described above.

Another approach is the direct modulation of amplitude and phase for each input light signal by an attenuator cooperated with a Soleil –Babinet compensator (SBC)[139] or a PID regulator[140]. In this scheme, the waveguide is a fixed and symmetric two-port Y-shape structure or a three-port structure, including a constant adjustment signal. The path lengths of the two branches are identical. The complex-amplitude modulation coefficients of input amplitude and phase for different types of logic gates are optimized to maximize the extinction between logic 0 and 1[139], shown in Table 2. It is assumed that the two logic gate input values are x_1 and x_2 (0 or 1). The logic gate output value is indicated by the light intensity of waveguide output $|\alpha x_1 + \beta x_2 + \gamma|^2$. Multimode interference is used to design logic gates with waveguides as well[143].

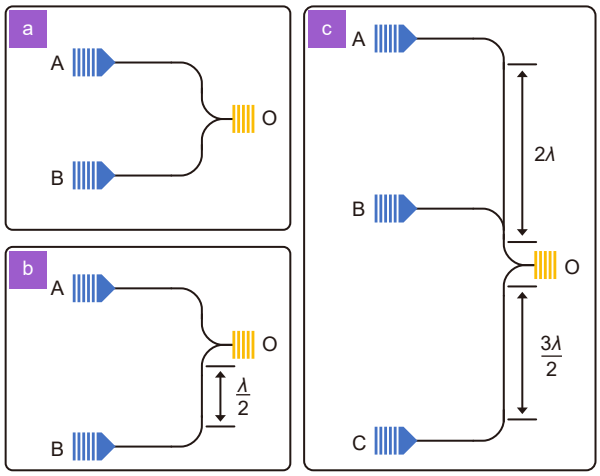

Fig. 12 | Optical logic gate based linear interference with waveguide path length differences: (**a**) OR gate; (**b**) XOR gate; (**c**) XNOR gate (A and B: input ports; O: output ports).

Periodically poled lithium niobates (PPLNs) waveguide

By comparison with conventional waveguides, a PPLN waveguide has the unique feature of cascaded second-harmonic generation and difference-frequency generation (SHG+DFG) if the quasi-phase matching (QPM) wavelength condition is satisfied[144–151]. When two data signals A and B with different frequencies are transmitted into the PPLN waveguide together with another continuous wave pump signal C, a new signal D at the sum of the frequencies will be generated due to SHG effect.

Table 2 | Optimized complex-amplitude modulation coefficients of input amplitude and phase for different types of logic gates. Table reproduced with permission from ref.[139], American Chemical Society.

Types of gates	Optimal parameters			Output light intensities for different input values				Output intensity contrast ratios
	α	β	γ	(0, 0)	(1, 0)	(0, 1)	(1, 1)	
OR	1	$e^{\frac{i2\pi}{3}}$	0	0	1	1	1	Infinity
AND	$\frac{2}{3}$	$\frac{2}{3}$	$-\frac{1}{3}$	$\frac{1}{9}$	$\frac{1}{9}$	$\frac{1}{9}$	1	9 : 1
NOT	1	0	−1	1	0	1	0	Infinity
NAND	1	$e^{\frac{i2\pi}{3}}$	$e^{-\frac{i2\pi}{3}}$	1	1	1	0	Infinity
NOR	$\frac{2}{3}$	$\frac{2}{3}$	−1	1	$\frac{1}{9}$	$\frac{1}{9}$	$\frac{1}{9}$	9 : 1
XOR	1	−1	0	0	1	1	0	Infinity
XNOR	1	1	−1	1	0	0	1	Infinity

Then it is simultaneously transformed into a pump signal C and a new idle signal E by DFG. Furthermore, the original signal A and B are depleted. An AND gate can be implemented easily by detecting the intensity of D or E when A and B are regarded as two input values. The output signals of two PPLN waveguides with A and B as input signals can be further combined in parallel through a coupler. Then a XOR gate can be realized by detecting the intensity of A (or B) alone in the output. If A and B are both present in the input ports, they will be depleted by SHG+DFG effect and disappear in the output. Nevertheless, A or B as the sole input can pass through the waveguide. The output of a PPLN waveguide with A and B as input signals can also be combined in parallel with the original input signal A, which can act as an OR gate by detecting A in the output. The trade-off is that PPLN needs to work under precise temperature control.

Microring resonator waveguide

A silicon microring resonator is typically coupled to a straight waveguide[152–161], as shown in Fig. 13. A resonance at a certain frequency f will be generated by this system. The output of the straight waveguide will be nearly zero when the microring resonates. If a pump pulse with sufficient power is applied, the refractive index of the microring will be changed by two-photon absorption (TPA) and the resonance frequency will increase (blue shift).

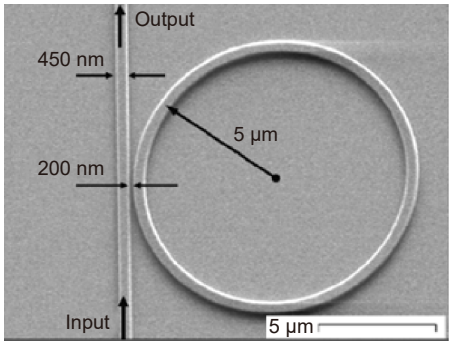

Fig. 13 | Microring resonator coupled with a straight waveguide with both pump signal and probe signal are injected into the input of the straight waveguide. Figure reproduced with permission from ref.[154], © The Optical Society.

Two input pump pulses A and B at another frequency can be designed so that one alone has insufficient power for blue shift but the sum of them reaches the power threshold for blue shift. When a probe light signal is initially tuned to a resonance, the output will be 0. When only A or B is 1, the output will still be 0. However, when both A and B are 1, the probe light will be out of resonance due to the blue shift of the resonant frequency. Consequently, the output will only be 1, in this case, making an AND gate.

Alternatively, the probe light is originally out of resonance at a frequency slightly smaller than f (output=1). Only when both A and B are 1 will the probe light be at resonance since the resonance frequency increases (output=0), resulting in a NAND operation.

In addition, AND and NAND gates can be implemented based on FWM instead of TPA[157]. In ref.[158], two symmetric microring resonators are cascaded, and the NOR gate is realized by producing an output signal of 0 at either resonance. By properly interconnecting multiple microring configurations[159], various logic gates such as NAND, AND, OR, and NOR can be realized. Its unique feature is that the input and output signals have the same wavelength (or frequency). Varying the resonant frequency between clockwise and counterclockwise propagating light signals can be employed in logic gate design as well[160].

Surface plasmon polariton (SPP)

SPP refers to electron oscillation at the interface between two materials excited by electrons or photons. SSP can overcome diffraction limits and reduce the size of bulky devices to densely integrated single chips. An SPP waveguide is commonly an air slot etched in a very thin metal film (e.g. gold or silver) on a silicon dioxide substrate. The reported device has a size less than 5 μm and can perform very precise phase control and ensure a high extinction ratio up to 24 dB[142]. The linear interference is commonly used to implement logic gates in an SPP waveguide[161–174,139,140,142]. The precision of phase modulation can be improved in various ways[162,166]. The coupling of optical signals can assist the design of logic gate as well[167,168]. A multifunctional and multichannel all-optical logic gate based on the in-plane coherent control of localized SPP is proposed in ref.[169]. An Au nanorod array is first placed on the Si substrate. Three plane-wave beams with the same wavelength including a TM-polarized control beam and two TE-polarized signal beams in opposite directions are coupled to the planar waveguide[169]. The output light intensities of nanorods at different spatial locations will provide different outputs for various logic gates.

Nanowire

Nanowires are another type of nanophotonic waveguide

device that can be used for optical logic gate computing[175–182]. The phase relationship of FWM in a single silicon nanowire can satisfy the requirement of an XOR logic gate[175,176], as with SOA and HNLF.

If the polarization and phase of input excitation lasers are properly controlled, the linear interference of plasmon signals allows the approximate implementation of AND, OR, XOR and NOT gate with a simple X or Y-shaped gold nanowire network[177], as shown in Fig. 14. NAND and NOR gates can be realized by cascading an AND gate (OR gate) and a NOT gate[177,178]. A common disadvantage of these nanowire schemes is that the extinction ratio between the output signal intensities for 1 and 0 is relatively low for some types of logic gates.

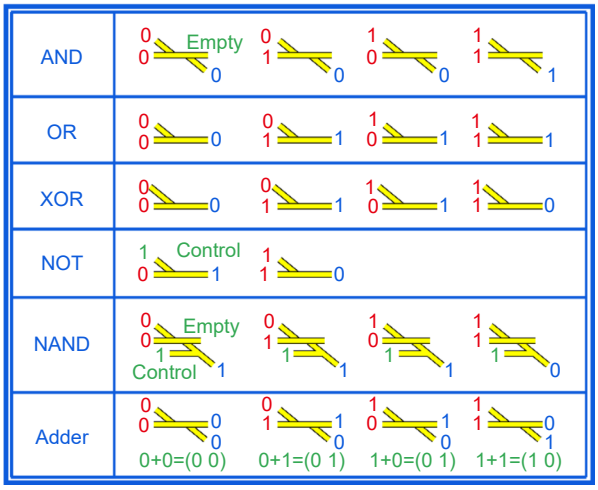

Fig. 14 | Simple nanowire networks for logic gates (input marked in red and output marked in blue). Figure reproduced with permission from ref.[177], American Chemical Society.

Photonic crystal structures

Photonic crystals are optical structures consisting of periodic geometric lattices. If the frequency of incident light lies within the photonic band gap, the light can be trapped in the photonic crystal structure. Two-dimensional photonic crystals such as a silicon substrate with etched dielectric holes or a system of dielectric rods in air are commonly used. The periodicity of dielectric functions in a photonic crystal can be broken by introducing point defects and line defects (removing or modifying some dielectric rods). Consequently, cavities and waveguides can be constructed within photonic crystals.

Several different effects in photonic crystals have been investigated[183,184] to implement optical logic gates including interference of self-collimated light[185–187], multi-mode interference (MMI)[188–190], coherent interference with phase difference, microring resonators and nonlinear effects.

Interference of self-collimated light

As an example of self-collimated light interference[185], a diagonal line defect is created by replacing the high refractive index dielectric rods with low refractive index air, as shown in Fig. 15. As a result, the incident light beams in both the horizontal and vertical directions will be partially reflected by the line defect and transmitted through the line defect. The collimated reflected and transmitted light beams can interfere constructively or destructively if an appropriate initial phase difference is set (e.g. $\pi/2$). The output light intensity in the horizontal or vertical direction can provide the correct logic gate output results (e.g. OR gate and XOR gate).

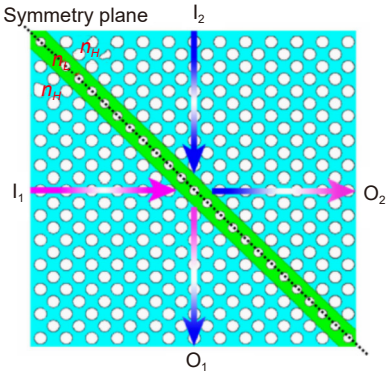

Fig. 15 | Self-collimated light interference in photonic crystals for logic gates (Input: I_1 and I_2, Output: O_1 or O_2)[185]. Figure reproduced with permission from ref.[185], © The Optical Society.

Multi-mode interference (MMI)

In a four-port system based on MMI[189] as shown in Fig. 16, when a light wave is launched into the input port, guided modes will be excited in the middle region connecting input ports and output ports, which propagate periodically in the propagation direction. When there is a certain phase difference between the input light waves of the two ports, the mode intensity distribution is more dense in the area close to one of the two output ports. In this case, one output port will have 1 and another output port will have 0. Four types of logic gates were investigated in ref.[189] with different phase settings. For example, a phase of 0 represents 1 and a phase of π represents 0 for Input 1, and a phase of $\pi/2$ represents 1 and a phase of $-\pi/2$ represents 0 for Input 2, when the system operates as an XOR gate. For convenience, the initial phase setting can be converted to a path length difference[190].

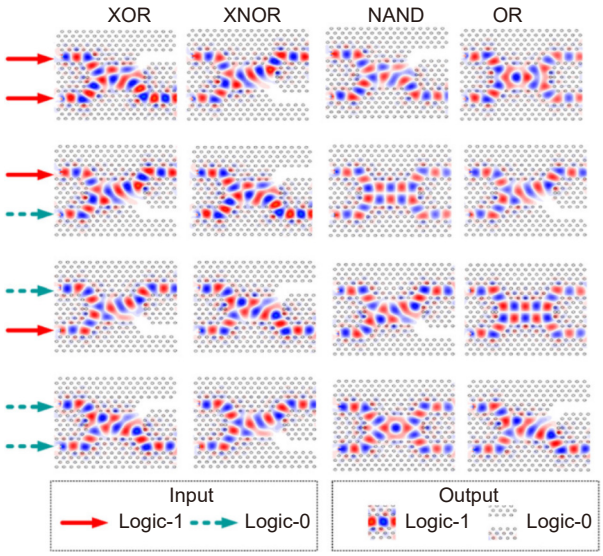

Fig. 16 | Logic gates based on MMI in a photonic crystal (input in the left and output in the right). Figure reproduced with permission from ref.[189], Elsevier.

Linear interference with phase difference

As in conventional waveguides, constructive and destructive linear interference between two input light signals with a phase difference of 0 or π enables logic gates to be designed in photonic crystals[191–200]. The phase difference can be generated by variation in path length, as shown in Fig. 17. Some point defects can be added to assist light propagation in the slot waveguide (line defect)[198–200].

Microring resonator structure

A microring resonator can be fabricated by removing dielectric rods in a photonic crystal. A microring placed near a slot waveguide can control whether light passes through the waveguide or not[201–211]. The coupling interactions between multiple slot waveguides and multiple microrings need to be taken into account[205–207,209–211]. The constructive and destructive interference of clockwise and counter-clockwise propagating signals within a microring is another critical design consideration[207,209]. In addition, a cavity can perform the same function as a microring[212].

In Fig. 18(a), a slot waveguide coupled with two microrings[201,203,204,208] can operate as either an AND gate or a NOR gate. The two control signals are regarded as Input A and Input B. If the microrings initially resonate, both control signals can change the resonant frequency and the probe light signal P with not be coupled with microrings. The light can pass the slot waveguide in the middle (AND gate). If the two original microrings are out of resonance, the two control signals can activate the microrings to couple with the probe signal (NOR gate).

In Fig. 18(b), for Input A, the light field is first induced by the top microring and then induced by the middle ring, including both clockwise and counterclockwise components. Consequently, the output will be 1 and the same can be applied to Input B. When both two input signals are activated, the signal interferes constructively at the output port (OR gate)[206]. However, if this symmetry is broken, destructive interference will yield other types of logic gates[207].

Nonlinear effects

Nonlinear Kerr medium can be inserted into the photonic crystal lattice to form a switch cavity[213–219]. The state of the switch can be changed if a control signal has a power over the threshold. Complementary photonic crystal integrated logic devices (CPCL) with universal logic gate integration capabilities are proposed. Examples of other approaches include topological cavity and edge states[220,221], FWM[129], coupling of neighboring cores in a photonic crystal fiber[222,223], MZI[224], Raman scattering[225], and 3D photonic structure with metamaterial[226].

Discussion, future prospect and conclusion

This paper reviewed achievements in the area of all-optical logic gate computing, where five different major types of schemes reported in the last decades were demonstrated and discussed, including spatial encoding of light fields, SOA, HNLF, microscale and nanoscale

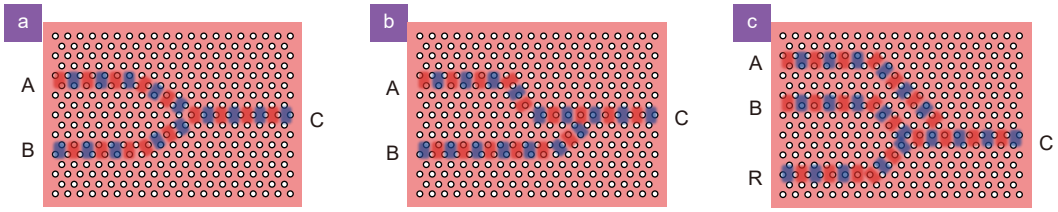

Fig. 17 | Linear interference with phase difference in photonic crystal: (**a**) OR gate; (**b**) XOR gate; (**c**) XNOR gate. Figure reproduced from ref.[192], Elsevier.

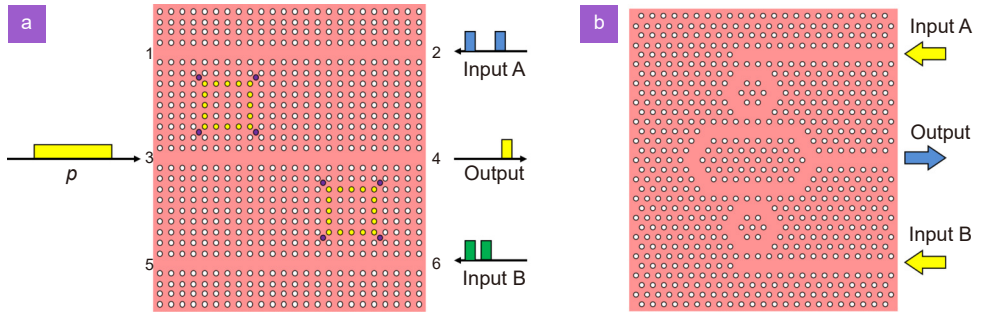

Fig. 18 | Two examples of microring structures in a photonic crystal: (**a**) AND gate (or NOR gate); (**b**) OR gate. Figure reproduced from: (a) ref.[204], Optical Society of America; (b) ref.[206], IEEE.

waveguides, and photonic crystal structures. All the methods presented above involve largely different working principles and present diverse advantages. Besides, other solutions are also reported in previous literature such as EIT effect[227,228], electro-optic effect with MZI[229–232], optical gradient force[233], vertical-cavity surface-emitting laser (VCSEL)[234,235] and black arsenic –phosphorus[236]. To sum up, a huge amount of macroscale, microscale and even nanoscale optical systems have proved to be potential candidates for all-optical logic gate systems. In practical experiments, Boolean logic rules can be implemented optically. Great progress has been made in the design of high-speed, compact, low-power-consumption and integrated all-optical logic gates. Although phased progress has been made, all-optical logic gates remain mainly at the laboratory research stage and still have a long way to go before industrial applications are realized.

At present, the capability of an optical logic gate computing system to perform logic functions is still insufficient for it to become a really viable option. In spite of this, several necessary requirements for a qualified logic gate have been proposed[237]. Firstly, the cascadability is a critical issue and a demonstration of individual logic gates without interconnections is inadequate. The format of the output optical signal must be consistent with the format of the input signal. For example, cascadability can be a challenging task if the input value is represented by light phase and the output value is represented by light intensity. Besides, the fan-out is a very important element. The output light signal of logic gate must be easily duplicated since it may be used to drive at least two further gates. Moreover, logic-level recovery needs to be taken into account. If the intermediate light signal in a logic gate network has an intensity (phase, polarization angle or others) that deviates from the predefined value for 1 or 0 due to fluctuation and noise, it needs to be restored otherwise the accumulated deviations will finally produce erroneous results. In addition, the isolation between inputs and outputs is critical. It is not desirable that the output of a logic gate feeds back to the input of the logic gate. Unfortunately, the feedback phenomenon is common in many optical systems. Furthermore, the system is required to have no critical biasing. It is undesirable that the system relies on very strict and precise conditions. However, optical systems often rely on high precision. For example, coherent light interference may need very precise separation distances between components to achieve accurate relative phases. Last but not least, the logic level shall be independent of loss. When a light signal propagates, it will inevitably suffer power loss and the logic level threshold between 0 and 1 will change, which mitigates against this requirement.

It is almost impossible to satisfy all these requirements in any of the optical logic gate schemes reviewed in this paper. There will be much space for further improvement from all these aspects in future works. In addition to the basic requirements stated above, optical logic gates are expected to demonstrate advantages over electronic logic gates in terms of common metrics such as speed of operation, device size, power efficiency and extinction ratio. More comparative studies between real electronic and optical logic gate systems can be conducted in future works.

In this paper, the authors mainly focus on all-optical logic gate computing. An alternative third approach in addition to all-optical logic gates and electronic logic gates is that electronics and photonics can be integrated for logic gate design[238–240]. The cooperation of electronics and photonics can be realized in various ways. One typical example is optical directed logic[238] where electronic signals are employed to control the status of optical switches to perform logic gate functions. In this case, the logic gates have electronic input signals and photonic

output signals. The optoelectronic logic gate schemes can combine the advantages of both optical computing and digital computing. They are relatively more consistent with the current electronic computing platforms. However, all-optical logic gate computing schemes are free of mutual conversion between electronic signals and optical signals. They can be directly applied to many optical sensing, communication and display applications. In addition, the inherent advantages of photonics over electronics can be better fully utilized by all-optical logic gates.

Nowadays, many research works only focus on the implementation of an individual optical logic gate. However, it is obvious that the implementation of a computer system or a logic circuit system for performing complex tasks (e.g. artificial intelligent tasks) is the final objective. A larger scale optical logic computing system can be attempted by using many individual logic gates as fundamental building blocks. At the moment, some devices consisting of multiple logic gates have been implemented such as a canonical logic units-based programmable logic array (CLUs-PLA)[241], half-adder and half-substractor[145,162,200,242], minterm[243], S-R flip-flop[244], divider circuit[245] and encoder & comparator[246]. At all events, more advanced systems remain to be further investigated in future. It is favorable that a photonic chip integrated with massive optical logic gates can be eventually implemented with novel silicon photonics technologies. Apart from building a universal optical computer, optical logic gates may exhibit their unique advantages in some specialized applications. In addition to the well-known all-optical signal processing application for fiber communications, other new application scenarios such as optical data storage[247] can be explored further.

Based on the discussions above, several additional comments for all-optical logic gate computing are given below. First, in electronic computing, individual logic gate components are implemented first and a more complicated logic circuit system is constructed with multiple individual gates. A large-scale logic computing system can be constructed by an assembly of small-scale logic computing blocks. Since serial interconnections and cascading of fundamental components can be easily accomplished in electronics, the "construct a building from bricks" mechanism stated above becomes a feasible option. But photonics supports more parallel multiplexing and less serial interconnection compared with electronics. In optical logic gate computing, it may not be necessary to exactly follow and replicate the electronic logic gate computing mechanism. Novel optical logic computing architectures can be developed[248]. For example, a complicated logic computing system can be modeled as a single "black box" in optics instead of being decomposed into more fundamental individual components. Second, in optical analogue computing, optical neural network has been extensively investigated in recent years and much progress has been made. A neural network consisting of many layers of neurons and a logic circuit computing system consisting of many interconnected individual logic gates have some similarity. They both involve linear weighted summation and nonlinear mathematical calculation. Binary neural networks have more common features than logic computing systems. In fact, a simple neural network can be used to model any type of logic gate or a basic logic circuit accurately. The bridge between optical analogue computing and optical logic gate computing may be built in future works. Third, in both optical analogue computing and optical logic gate computing, the lack of optimal nonlinear optical elements is a critical challenge. In optical neural network, the linear weight summation calculation can be realized successfully in several different ways. But all-optical nonlinear activation functions are much more difficult to realize. For microscale and nanoscale optical logic gates with on-chip waveguides and photonic crystal structures, linear interference of coherent light signals is one approach but it has several limitations. The nonlinear optical effects are more promising. However, currently, there is almost no ideal optical nonlinear effect with simultaneous low-power excitation, fast response and easy implementation. This obstacle hinders the development of optical logic gate, optical neural network and other optical computing research works. The investigation on emerging highly nonlinear optical materials[249,250] may open up new potential opportunities.

It has to be pointed out that significant achievements have been made in the field of all-optical logic gate design in recent decades. While, a number of critical challenges are yet to be overcome before the technology can move from the laboratory into a real world of complicated environment in the future, the exploration of new materials and systems will be an effective way to improve an all-optical logic gate computing system. It can be predicted that with further research, there will be more powerful and more practical all-optical logic gate computing systems.

References

1. Wu JM, Lin X, Guo YC, Liu JW, Fang L et al. Analog optical computing for artificial intelligence. *Engineering* **10**, 133–145 (2022).
2. Liu J, Wu QH, Sui XB, Chen Q, Gu GH et al. Research progress in optical neural networks: theory, applications and developments. *PhotoniX* **2**, 5 (2021).
3. Xu RQ, Lv P, Xu FJ, Shi YS. A survey of approaches for implementing optical neural networks. *Opt Laser Technol* **136**, 106787 (2021).
4. Wetzstein G, Ozcan A, Gigan S, Fan SH, Englund D et al. Inference in artificial intelligence with deep optics and photonics. *Nature* **588**, 39–47 (2020).
5. Sui XB, Wu QH, Liu J, Chen Q, Gu GH. A review of optical neural networks. *IEEE Access* **8**, 70773–70783 (2020).
6. De Marinis L, Cococcioni M, Castoldi P, Andriolli N. Photonic neural networks: a survey. *IEEE Access* **7**, 175827–175841 (2019).
7. Shen YC, Harris NC, Skirlo S, Prabhu M, Baehr-Jones T et al. Deep learning with coherent nanophotonic circuits. *Nat Photonics* **11**, 441–446 (2017).
8. Feldmann J, Youngblood N, Karpov M, Gehring H, Li X et al. Parallel convolutional processing using an integrated photonic tensor core. *Nature* **589**, 52–58 (2021).
9. Lin X, Rivenson Y, Yardimci NT, Veli M, Luo Y et al. All-optical machine learning using diffractive deep neural networks. *Science* **361**, 1004–1008 (2018).
10. Zuo Y, Li BH, Zhao YJ, Jiang Y, Chen YC et al. All-optical neural network with nonlinear activation functions. *Optica* **6**, 1132–1137 (2019).
11. Jiao SM, Feng J, Gao Y, Lei T, Xie ZW et al. Optical machine learning with incoherent light and a single-pixel detector. *Opt Lett* **44**, 5186–5189 (2019).
12. Zuo Y, Zhao YJ, Chen YC, Du SW, Liu JW. Scalability of all-optical neural networks based on spatial light modulators. *Phys Rev Appl* **15**, 054034 (2021).
13. Tait AN, De Lima TF, Zhou E, Wu AX, Nahmias MA et al. Neuromorphic photonic networks using silicon photonic weight banks. *Sci Rep* **7**, 7430 (2017).
14. Huang CR, Bilodeau S, De Lima TF, Tait AN, Ma PY et al. Demonstration of scalable microring weight bank control for large-scale photonic integrated circuits. *APL Photonics* **5**, 040803 (2020).
15. Xu XY, Tan MX, Corcoran B, Wu JY, Boes A et al. 11 TOPS photonic convolutional accelerator for optical neural networks. *Nature* **589**, 44–51 (2021).
16. Khoram E, Chen A, Liu DJ, Ying L, Wang QQ et al. Nanophotonic media for artificial neural inference. *Photonics Res* **7**, 823–827 (2019).
17. Liao K, Chen Y, Yu ZC, Hu XY, Wang XY et al. All-optical computing based on convolutional neural networks. *Opto-Electron Adv* **4**, 200060 (2021).
18. Davoodi F, Granpayeh N. All optical logic gates: a tutorial. *Int J Inf Commun Technol Res* **4**, 65–98 (2012).
19. Singh P, Tripathi DK, Jaiswal S, Dixit HK. All-optical logic gates: designs, classification, and comparison. *Adv Opt Technol* **2014**, 275083 (2014).
20. Sasikala V, Chitra K. All optical switching and associated technologies: a review. *J Opt* **47**, 307–317 (2018).
21. Saharia A, Mudgal N, Agarwal A, Sahu S, Jain S et al. A comparative study of various all-optical logic gates. In *Optical and Wireless Technologies* 429–437 (Springer, Singapore, 2020); https://doi.org/10.1007/978-981-13-6159-3_45.
22. Minzioni P, Lacava C, Tanabe T, Dong JJ, Hu XY et al. Roadmap on all-optical processing. *J Opt* **21**, 063001 (2019).
23. Wang J, Long Y. On-chip silicon photonic signaling and processing: a review. *Sci Bull* **63**, 1267–1310 (2018).
24. Ghaffari BM, Salehi JA. Multiclass, multistage, and multilevel fiber-optic CDMA signaling techniques based on advanced binary optical logic gate elements. *IEEE Trans Commun* **57**, 1424–1432 (2009).
25. Asakawa K, Sugimoto Y, Nakamura S. Silicon photonics for telecom and data-com applications. *Opto-Electron Adv* **3**, 200011 (2020).
26. Caulfield HJ, Westphal J. The logic of optics and the optics of logic. *Inf Sci* **162**, 21–33 (2004).
27. Qian L, Caulfield HJ. What can we do with a linear optical logic gate. *Inf Sci* **176**, 3379–3392 (2006).
28. Tanida J, Ichioka Y. Optical logic array processor using shadowgrams. *J Opt Soc Am* **73**, 800–809 (1983).
29. Ichioka Y, Tanida J. Optical parallel logic gates using a shadow-casting system for optical digital computing. *Proc IEEE* **72**, 787–801 (1984).
30. Yatagai T. Optical space-variant logic-gate array based on spatial encoding technique. *Opt Lett* **11**, 260–262 (1986).
31. Li Y, Eichmann G, Alfano RR. Optical computing using hybrid encoded shadow casting. *Appl Opt* **25**, 2636–2638 (1986).
32. Jutamulia S, Storti G. Noncoded shadow-casting logic array. *Appl Opt* **28**, 4517–4518 (1989).
33. Yamamoto H, Hayasaki Y, Nishida N. Securing information display by use of visual cryptography. *Opt Lett* **28**, 1564–1566 (2003).
34. Shi YS, Yang XB. Optical hiding with visual cryptography. *J Opt* **19**, 115703 (2017).
35. Jiao SM, Feng J, Gao Y, Lei T, Yuan XC. Visual cryptography in single-pixel imaging. *Opt Express* **28**, 7301–7313 (2020).
36. Karim MA, Awwal AAS, Cherri AK. Polarization-encoded optical shadow-casting logic units: design. *Appl Opt* **26**, 2720–2725 (1987).
37. Lohmann AW, Weigelt J. Spatial filtering logic based on polarization. *Appl Opt* **26**, 131–135 (1987).
38. Lohmann AW. Polarization and optical logic. *Appl Opt* **25**, 1594–1597 (1986).
39. Torroba R, Henao R, Carletti C. Digital polarization-encoding technique for optical logic operations. *Opt Lett* **21**, 1918–1920 (1996).
40. Zaghloul YA, Zaghloul ARM. Unforced polarization-based optical implementation of Binary logic. *Opt Express* **14**, 7252–7269 (2006).
41. Zaghloul YA, Zaghloul ARM. Complete all-optical processing polarization-based binary logic gates and optical processors. *Opt Express* **14**, 9879–9895 (2006).
42. Zaghloul YA, Zaghloul ARM, Adibi A. Passive all-optical polarization switch, binary logic gates, and digital processor. *Opt Express* **19**, 20332–20346 (2011).
43. Qian C, Lin X, Lin XB, Xu J, Sun Y et al. Performing optical logic operations by a diffractive neural network. *Light Sci Appl* **9**, 59 (2020).
44. Zhao ZH, Wang Y, Ding XM, Li HY, Fu JH et al. Compact lo-

gic operator utilizing a single-layer metasurface. *Photonics Res* **10**, 316–322 (2022).
45. Wang PP, Xiong WJ, Huang ZB, He YL, Xie ZQ et al. Orbital angular momentum mode logical operation using optical diffractive neural network. *Photonics Res* **9**, 2116–2124 (2021).
46. Jenkins BK, Sawchuk AA, Strand TC, Forchheimer R, Soffer BH. Sequential optical logic implementation. *Appl Opt* **23**, 3455–3464 (1984).
47. Stubkjaer KE. Semiconductor optical amplifier-based all-optical gates for high-speed optical processing. *IEEE J Select Top Quant Electron* **6**, 1428–1435 (2000).
48. Zhang M, Wang L, Ye PD. All optical XOR logic gates: technologies and experiment demonstrations. *IEEE Commun Mag* **43**, S19–S24 (2005).
49. Hamie A, Sharaiha A, Guegan M, Pucel B. All-optical Logic NOR gate using two-cascaded semiconductor optical amplifiers. *IEEE Photonics Technol Lett* **14**, 1439–1441 (2002).
50. Kim JH, Kim YI, Byun YT, Jhon YM, Lee S et al. All-optical logic gates using semiconductor optical-amplifier-based devices and their applications. *J Korean Phys Soc* **45**, 1158–1161 (2004).
51. Kim SH, Kim JH, Yu BG, Byun YT, Jeon YM et al. All-optical NAND gate using cross-gain modulation in semiconductor optical amplifiers. *Electron Lett* **41**, 1027–1028 (2005).
52. Sharaiha A, Topomondzo J, Morel P. All-optical logic AND–NOR gate with three inputs based on cross-gain modulation in a semiconductor optical amplifier. *Opt Commun* **265**, 322–325 (2006).
53. Sasikala V, Chitra K. Performance analysis of multilogic all-optical structure based on nonlinear signal processing in SOA. *J Opt* **49**, 208–215 (2020).
54. Kim JH, Jhon YM, Byun YT, Lee S, Woo DH et al. All-optical XOR gate using semiconductor optical amplifiers without additional input beam. *IEEE Photonics Technol Lett* **14**, 1436–1438 (2002).
55. Dong JJ, Zhang XL, Xu J, Huang DX. 40 Gb/s all-optical logic NOR and OR gates using a semiconductor optical amplifier: Experimental demonstration and theoretical analysis. *Opt Commun* **281**, 1710–1715 (2008).
56. Dong JJ, Zhang XL, Huang DX. A proposal for two-input arbitrary Boolean logic gates using single semiconductor optical amplifier by picosecond pulse injection. *Opt Express* **17**, 7725–7730 (2009).
57. Kumar S, Willner AE. Simultaneous four-wave mixing and cross-gain modulation for implementing an all-optical XNOR logic gate using a single SOA. *Opt Express* **14**, 5092–5097 (2006).
58. Wu BB, Fu SN, Wu J, Shum P, Ngo NQ et al. Simultaneous implementation of all-optical OR and AND logic gates for NRZ/RZ/CSRZ ON –OFF-keying signals. *Opt Commun* **283**, 349–354 (2010).
59. Li ZH, Li GF. Ultrahigh-speed reconfigurable logic gates based on four-wave mixing in a semiconductor optical amplifier. *IEEE Photonics Technol Lett* **18**, 1341–1343 (2006).
60. Chan K, Chan CK, Chen LK, Tong F. Demonstration of 20-Gb/s all-optical XOR gate by four-wave mixing in semiconductor optical amplifier With RZ-DPSK modulated inputs. *IEEE Photonics Technol Lett* **16**, 897–899 (2004).
61. Kang I, Dorrer C, Leuthold J. All-optical XOR operation of 40 Gbit/s phase-shift-keyed data using four-wave mixing in semiconductor optical amplifier. *Electron Lett* **40**, 496–498 (2004).
62. Deng N, Chan K, Chan CK, Chen LK. An all-optical XOR logic gate for high-speed RZ-DPSK signals by FWM in semiconductor optical amplifier. *IEEE J Select Top Quant Electron* **12**, 702–707 (2006).
63. Kong DM, Li Y, Wang H, Zhang XP, Zhang JY et al. All-optical XOR gates for QPSK signals based on four-wave mixing in a semiconductor optical amplifier. *IEEE Photonics Technol Lett* **24**, 988–990 (2012).
64. Berrettini G, Simi A, Malacarne A, Bogoni A, Poti L. Ultrafast integrable and reconfigurable XNOR, AND, NOR, and NOT photonic logic gate. *IEEE Photonics Technol Lett* **18**, 917–919 (2006).
65. Dong J, Zhang X, Wang Y, Xu J, Huang D. 40 Gbit/s reconfigurable photonic logic gates based on various nonlinearities in single SOA. *Electron Lett* **43**, 884–886 (2007).
66. Dong JJ, Zhang XL, Fu SN, Xu J, Shum P et al. Ultrafast all-optical signal processing based on single semiconductor optical amplifier and optical filtering. *IEEE J Select Top Quant Electron* **14**, 770–778 (2008).
67. Chen X, Huo L, Zhao ZX, Zhuang L, Lou CY. Reconfigurable all-optical logic gates using single semiconductor optical amplifier at 100-Gb/s. *IEEE Photonics Technol Lett* **28**, 2463–2466 (2016).
68. Han BC, Liu Y. All-optical reconfigurable non-inverted logic gates with a single semiconductor optical amplifier. *AIP Adv* **9**, 015007 (2019).
69. Soto H, Erasme D, Guekos G. 5-Gb/s XOR optical gate based on cross-polarization modulation in semiconductor optical amplifiers. *IEEE Photonics Technol Lett* **13**, 335–337 (2001).
70. Guo LQ, Connelly MJ. All-optical AND gate with improved extinction ratio using signal induced nonlinearities in a bulk semiconductor optical amplifier. *Opt Express* **14**, 2938–2943 (2006).
71. Zhang JY, Wu J, Feng CF, Xu K, Lin JT. All-optical logic OR gate exploiting nonlinear polarization rotation in an SOA and red-shifted sideband filtering. *IEEE Photonics Technol Lett* **19**, 33–35 (2007).
72. Han LY, Wen H, Jiang H, Guo YL, Zhang HY. All-Optical AND logic gate without additional input beam by utilizing cross polarization modulation effect. *Chin Phys Lett* **25**, 3901–3904 (2008).
73. Mukherjee K, Raja A, Maji K. All-optical logic gate NAND using semiconductor optical amplifiers with simulation. *J Opt* **48**, 357–364 (2019).
74. Toliver P, Runser RJ, Glesk I, Prucnal PR. Comparison of three nonlinear interferometric optical switch geometries. *Opt Commun* **175**, 365–373 (2000).
75. Fjelde T, Wolfson D, Kloch A, Dagens B, Coquelin A et al. Demonstration of 20 Gbit/s all-optical logic XOR in integrated SOA-based interferometric wavelength converter. *Electron Lett* **36**, 1863–1864 (2000).
76. Wang Q, Zhu GH, Chen HM, Jaques J, Leuthold J et al. Study of all-optical XOR using Mach–Zehnder interferometer and differential scheme. *IEEE J Quant Electron* **40**, 703–710 (2004).
77. Sun HZ, Wang Q, Dong H, Chen Z, Dutta NK et al. All-Optical logic XOR gate at 80 Gb/s using SOA-MZI-DI. *IEEE J Quant Electron* **42**, 747–751 (2006).
78. Dailey JM, Webb RP, Manning RJ. All-optical technique for modulation format conversion from on-off-keying to alternate-

mark-inversion. *Opt Express* **18**, 21873–21882 (2010).
79. Dong H, Sun H, Wang Q, Dutta NK, Jaques J. 80 Gb/s All-optical logic AND operation using Mach-Zehnder interferometer with differential scheme. *Opt Commun* **265**, 79–83 (2006).
80. Wang G, Yang XL, Hu WS. All-optical logic gates for 40Gb/s NRZ signals using complementary data in SOA-MZIs. *Opt Commun* **290**, 28–32 (2013).
81. Taraphdar C, Chattopadhyay T, Roy JN. Mach–Zehnder interferometer-based all-optical reversible logic gate. *Opt Laser Technol* **42**, 249–259 (2010).
82. Kang I, Rasras M, Buhl L, Dinu M, Cabot S et al. All-optical XOR and XNOR operations at 86.4 Gb/s using a pair of semiconductor optical amplifier Mach-Zehnder interferometers. *Opt Express* **17**, 19062–19066 (2009).
83. Kim JY, Kang JM, Kim TY, Han SK. All-Optical multiple logic gates with XOR, NOR, OR, and NAND functions using parallel SOA-MZI structures: theory and experiment. *J Lightwave Technol* **24**, 3392–3399 (2006).
84. Kotb A, Zoiros KE, Guo CL. All-optical XOR, NOR, and NAND logic functions with parallel semiconductor optical amplifier-based Mach-Zehnder interferometer modules. *Opt Laser Technol* **108**, 426–433 (2018).
85. Kotb A, Guo CL. 100 Gb/s all-optical multifunctional AND, NOR, XOR, OR, XNOR, and NAND logic gates in a single compact scheme based on semiconductor optical amplifiers. *Opt Laser Technol* **137**, 106828 (2021).
86. Zhang M, Zhao YP, Wang L, Wang J, Ye PD. Design and analysis of all-optical XOR gate using SOA-based Mach–Zehnder interferometer. *Opt Commun* **223**, 301–308 (2003).
87. Houbavlis T, Zoiros KE, Kanellos G, Tsekrekos C. Performance analysis of ultrafast all-optical Boolean XOR gate using semiconductor optical amplifier-based Mach–Zehnder Interferometer. *Opt Commun* **232**, 179–199 (2004).
88. Ye XH, Ye PD, Zhang M. All-optical NAND gate using integrated SOA-based Mach –Zehnder interferometer. *Opt Fiber Technol* **12**, 312–316 (2006).
89. Sokoloff JP, Prucnal PR, Glesk I, Kane M. A terahertz optical asymmetric demultiplexer (TOAD). *IEEE Photonics Technol Lett* **5**, 787–790 (1993).
90. Houbavlis T, Zoiros K, Hatziefremidis A, Avramopoulos H, Occhi L et al. 10 Gbit/s all-optical Boolean XOR with SOA fibre Sagnac gate. *Electron Lett* **35**, 1650–1652 (1999).
91. Zhou YF, Wu J, Lin JT. Novel ultrafast all-optical XOR scheme based on Sagnac interferometric structure. *IEEE J Quant Electron* **41**, 823–827 (2005).
92. Zoiros KE, Papadopoulos G, Houbavlis T, Kanellos GT. Theoretical analysis and performance investigation of ultrafast all-optical Boolean XOR gate with semiconductor optical amplifier-assisted Sagnac interferometer. *Opt Commun* **258**, 114–134 (2006).
93. Feng CF, Wu J, Xu K, Lin JT. Simple ultrafast all-optical AND logic gate. *Opt Eng* **46**, 125006 (2007).
94. Chattopadhyay T, Roy JN. Semiconductor optical amplifier (SOA)-assisted Sagnac switch for designing of all-optical TRI-state logic gates. *Optik* **122**, 1073–1078 (2011).
95. Roy JN, Gayen DK. Integrated all-optical logic and arithmetic operations with the help of a TOAD-based interferometer device-alternative approach. *Appl Opt* **46**, 5304–5310 (2007).
96. Bintjas C, Kalyvas M, Theophilopoulos G, Stathopoulos T, Avramopoulos H et al. 20 Gb/s all-optical XOR with UNI gate. *IEEE Photonics Technol Lett* **12**, 834–836 (2000).
97. Webb RP, Yang X, Manning RJ, Giller R. All-optical 40 Gbit/s XOR gate with dual ultrafast nonlinear interferometer. *Electron Lett* **41**, 1396–1397 (2005).
98. Siarkos T, Zoiros KE, Nastou D. On the feasibility of full pattern-operated all-optical XOR gate with single semiconductor optical amplifier-based ultrafast nonlinear interferometer. *Opt Commun* **282**, 2729–2440 (2009).
99. Dong H, Wang Q, Zhu G, Jaques J, Piccirilli AB et al. Demonstration of all-optical logic OR gate using semiconductor optical amplifier-delayed interferometer. *Opt Commun* **242**, 479–485 (2004).
100. Wang Q, Dong H, Zhu G, Sun H, Jaques J et al. All-optical logic OR gate using SOA and Delayed interferometer. *Opt Commun* **260**, 81–86 (2006).
101. Xu J, Zhang XL, Zhang Y, Dong JJ, Liu DM et al. Reconfigurable all-optical logic gates for multi-input differential phase-shift keying signals: design and experiments. *J Lightwave Technol* **27**, 5268–5275 (2009).
102. Zhao XF, Lou CY, Feng YM. Optical signal processing based on semiconductor optical amplifier and tunable delay interferometer. *Front Optoelectron China* **4**, 308–314 (2011).
103. Dong WC, Huang ZY, Hou J, Santos R, Zhang XL. Integrated all-optical programmable logic array based on semiconductor optical amplifiers. *Opt Lett* **43**, 2150–2153 (2018).
104. Ma SZ, Chen Z, Dutta NK. All-optical logic gates based on two-photon absorption in semiconductor optical amplifiers. *Opt Commun* **282**, 4508–4012 (2009).
105. Ma SZ, Chen Z, Sun HZ, Dutta NK. High speed all optical logic gates based on quantum dot semiconductor optical amplifiers. *Opt Express* **18**, 6417–6422 (2010).
106. Rostami A, Nejad HBA, Qartavol RM, Saghai HR. Tb/s optical logic gates based on quantum-dot semiconductor optical amplifiers. *IEEE J Quant Electron* **46**, 354–360 (2010).
107. Dimitriadou E, Zoiros KE. On the design of ultrafast all-optical NOT gate using quantum-dot semiconductor optical amplifier-based Mach –Zehnder interferometer. *Opt Laser Technol* **44**, 600–607 (2012).
108. Kotb A. Simulation of high quality factor all-optical logic gates based on quantum-dot semiconductor optical amplifier at 1 Tb/s. *Optik* **127**, 320–325 (2016).
109. Zhang X, Dutta NK. Effects of two-photon absorption on all optical logic operation based on quantum-dot semiconductor optical amplifiers. *J Mod Opt* **65**, 166–173 (2018).
110. Hu HY, Zhang X, Zhao S. High-speed all optical logic gate using QD-SOA and its application. *Cogent Phys* **4**, 1388156 (2017).
111. Kotb A, Zoiros KE, Guo CL. 2 Tb/s all-optical gates based on two-photon absorption in quantum dot semiconductor optical amplifiers. *Opt Laser Technol* **112**, 442–451 (2019).
112. Kotb A, Guo CL. All-optical NOR and XNOR logic gates at 2 Tb/s based on two-photon absorption in quantum-dot semiconductor optical amplifiers. *Opt Quant Electron* **52**, 30 (2020).
113. Kotb A, Guo CL. 120 Gb/s all-optical NAND logic gate using reflective semiconductor optical amplifiers. *J Mod Opt* **67**, 1138–1144 (2020).
114. Kotb A, Guo CL. Numerical modeling of photonic crystal semiconductor optical amplifiers-based 160 Gb/s all-optical NOR and XNOR logic gates. *Opt Quant Electron* **52**, 89 (2020).
115. Kwok CH, Lin C. Polarization-insensitive all-optical NRZ-to-RZ

format conversion by spectral filtering of a cross phase modulation broadened signal spectrum. *IEEE J Select Top Quant Electron* **12**, 451–458 (2006).
116. Bogris A, Velanas P, Syvridis D. Numerical investigation of a 160-Gb/s reconfigurable photonic logic gate based on cross-phase modulation in fibers. *IEEE Photonics Technol Lett* **19**, 402–404 (2007).
117. Qiu JF, Sun K, Rochette M, Chen LR. Reconfigurable all-optical multilogic gate (XOR, AND, and OR) based on cross-phase modulation in a highly nonlinear fiber. *IEEE Photonics Technol Lett* **22**, 1199–1201 (2010).
118. Bogoni A, Potì L, Proietti R, Meloni G, Ponzini F et al. Regenerative and reconfigurable all-optical logic gates for ultra-fast applications. *Electron Lett* **41**, 435–436 (2005).
119. Miyoshi Y, Ikeda K, Tobioka H, Inoue T, Namiki S et al. Ultra-fast all-optical logic gate using a nonlinear optical loop mirror based multi-periodic transfer function. *Opt Express* **16**, 2570–2577 (2008).
120. Lai DMF, Kwok CH, Wong KKY. All-optical picoseconds logic gates based on a fiber optical parametric amplifier. *Opt Express* **16**, 18362–18370 (2008).
121. Li LL, Wu J, Qiu JF, Wu BB, Xu K et al. Reconfigurable all-optical logic gate using four-wave mixing (FWM) in HNLF for NRZ-PolSK signal. *Opt Commun* **283**, 3608–3612 (2010).
122. Wang J, Sun QZ, Sun JQ. All-optical 40 Gbit/s CSRZ-DPSK logic XOR gate and format conversion using four-wave mixing. *Opt Express* **17**, 12555–12563 (2009).
123. Fagotto EAM, Abbade MLF. All-optical demultiplexing of 4-ASK optical signals with four-wave mixing optical gates. *Opt Commun* **283**, 1102–1109 (2010).
124. Yu CY, Christen L, Luo T, Wang Y, Pan ZQ et al. All-optical XOR gate using polarization rotation in single highly nonlinear fiber. *IEEE Photonics Technol Lett* **17**, 1232–1234 (2005).
125. Chen Y, Cheng YK, Zhu RB, Wang FF, Cheng HT et al. Nanoscale all-optical logic devices. *Sci China Phys Mech Astron* **62**, 44201 (2019).
126. Wang LJ, Yan LS, Guo YH, Wen KH, Pan W et al. Optical quasi logic gates based on polarization-dependent four-wave mixing in subwavelength metallic waveguides. *Opt Express* **21**, 14442–14451 (2013).
127. Gao SM, Wang XY, Xie YQ, Hu PR, Yan Q. Reconfigurable dual-channel all-optical logic gate in a silicon waveguide using polarization encoding. *Opt Lett* **40**, 1448–1451 (2015).
128. Vo TD, Pant R, Pelusi MD, Schröder J, Choi DY et al. Photonic chip-based all-optical XOR gate for 40 and 160 Gbit/s DPSK signals. *Opt Lett* **36**, 710–712 (2011).
129. Husko C, Vo TD, Corcoran B, Li J, Krauss TF et al. Ultracompact all-optical XOR logic gate in a slow-light silicon photonic crystal waveguide. *Opt Express* **19**, 20681–20690 (2011).
130. Liang TK, Nunes LR, Tsuchiya M, Abedin KS, Miyazaki T et al. High speed logic gate using two-photon absorption in silicon waveguides. *Opt Commun* **265**, 171–174 (2006).
131. Wu W, Sun QB, Wang LR, Wang GX, Zeng C et al. Influence of two-photon absorption and free-carrier effects on all-optical logic gates in silicon waveguides. *Appl Phys Express* **12**, 042005 (2019).
132. Passaro VMN, De Passaro F. All-optical AND gate based on Raman effect in silicon-on-insulator waveguide. *Opt Quant Electron* **38**, 877–888 (2006).
133. Khorasaninejad M, Saini SS. All-optical logic gates using nonlinear effects in silicon-on-insulator waveguides. *Appl Opt* **48**, F31–F36 (2009).
134. Fujisawa T, Koshiba M. All-optical logic gates based on nonlinear slot-waveguide couplers. *J Opt Soc Am B* **23**, 684–691 (2006).
135. Larom B, Nazarathy M, Rudnitsky A, Nevet A, Zalevsky Z. Cascadable and reconfigurable photonic logic gates based on linear Lightwave interference and non-linear phase erasure. *Opt Express* **18**, 13600–13607 (2010).
136. Pan D, Wei H, Xu HX. Optical interferometric logic gates based on metal slot waveguide network realizing whole fundamental logic operations. *Opt Express* **21**, 9556–9562 (2013).
137. Lu QC, Yan X, Wei W, Zhang X, Zhang MQ et al. High-speed ultra-compact all-optical NOT and AND logic gates designed by a multi-objective particle swarm optimized method. *Opt Laser Technol* **116**, 322–327 (2019).
138. Yao CN, Kotb A, Wang B, Singh SC, Guo CL. All-optical logic gates using dielectric-loaded waveguides with quasi-rhombus metasurfaces. *Opt Lett* **45**, 3769–3772 (2020).
139. Peng CN, Li JY, Liao HM, Li Z, Sun CW et al. Universal linear-optical logic gate with maximal intensity contrast ratios. *ACS Photonics* **5**, 1137–1143 (2018).
140. Kita S, Nozaki K, Takata K, Shinya A, Notomi M. Ultrashort low-loss Ψ gates for linear optical logic on Si photonics platform. *Commun Phys* **3**, 33 (2020).
141. Ortiz-Martinez M, Hernandez-Serrano AI, Guerrero MAJ, Strupiechonski E, Castro-Camus E. Logic gates for terahertz frequencies fabricated by three-dimensional printing. *J Opt Soc Am B* **37**, 3660–3664 (2020).
142. Fu YL, Hu XY, Lu CC, Yue S, Yang H et al. All-optical logic gates based on nanoscale plasmonic slot waveguides. *Nano Lett* **12**, 5784–5790 (2012).
143. Li ZJ, Chen ZW, Li BJ. Optical pulse controlled all-optical logic gates in SiGe/Si multimode interference. *Opt Express* **13**, 1033–1038 (2005).
144. Lee YL, Yu BA, Eom TJ, Shin W, Jung C et al. All-optical AND and NAND gates based on cascaded second-order nonlinear processes in a Ti-diffused periodically poled $LiNbO_3$ waveguide. *Opt Express* **14**, 2776–2782 (2006).
145. Wang J, Sun JQ, Sun QZ. Single-PPLN-based simultaneous half-adder, half-subtracter, and OR logic gate: proposal and simulation. *Opt Express* **15**, 1690–1699 (2007).
146. Wang J, Sun JQ, Sun QZ, Wang DL, Zhou MJ et al. All-optical format conversion using a periodically poled lithium niobate waveguide and a reflective semiconductor optical amplifier. *Appl Phys Lett* **91**, 051107 (2007).
147. Wang J, Sun JQ, Sun QZ, Wang DL, Zhou MJ et al. Experimental observation of all-optical non-return-to-zero-to-return-to-zero format conversion based on cascaded second-order nonlinearity assisted by active mode-locking. *Opt Lett* **32**, 2462–2464 (2007).
148. McGeehan JE, Giltrelli M, Willner AE. All-optical digital 3-input AND gate using sum- and difference-frequency generation in PPLN waveguide. *Electron Lett* **43**, 409–410 (2007).
149. Wang J, Sun JQ, Zhang XL, Huang DX, Fejer MM. Ultrafast all-optical three-input Boolean XOR operation for differential phase-shift keying signals using periodically poled lithium niobate. *Opt Lett* **33**, 1419–1421 (2008).
150. Wang J, Sun JQ, Sun QZ, Wang DL, Zhang XL et al. PPLN-based flexible optical logic AND gate. *IEEE Photonics Technol*

Lett **20**, 211–213 (2008).
151. Bogoni A, Wu XX, Bakhtiari Z, Nuccio S, Willner AE. 640 Gbits/s photonic logic gates. *Opt Lett* **35**, 3955–3957 (2010).
152. Ibrahim TA, Grover R, Kuo LC, Kanakaraju S, Calhoun LC et al. All-optical AND/NAND logic gates using semiconductor microresonators. *IEEE Photonics Technol Lett* **15**, 1422–1424 (2003).
153. Almeida VR, Barrios CA, Panepucci RR, Lipson M. All-optical control of light on a silicon chip. *Nature* **431**, 1081–1084 (2004).
154. Xu QF, Lipson M. All-optical logic based on silicon micro-ring resonators. *Opt Express* **15**, 924–929 (2007).
155. Zhao WY, Ju DQ, Jiang YY. Pulse controlled all-optical logic gate based on nonlinear ring resonator realizing all fundamental logic operations. *Plasmonics* **10**, 311–317 (2015).
156. Moradi M, Danaie M, Orouji AA. Design of all-optical XOR and XNOR logic gates based on Fano resonance in plasmonic ring resonators. *Opt Quant Electron* **51**, 154 (2019).
157. Mikroulis S, Simos H, Roditi E, Chipouras A, Syvridis D. 40-Gb/s NRZ and RZ operation of an all-optical AND logic gate based on a passive InGaAsP/InP microring resonator. *J Lightwave Technol* **24**, 1159–1164 (2006).
158. Ibrahim TA, Amarnath K, Kuo LC, Grover R, Van V et al. Photonic logic NOR gate based on two symmetric microring resonators. *Opt Lett* **29**, 2779–2781 (2004).
159. Fushimi A, Tanabe T. All-optical logic gate operating with single wavelength. *Opt Express* **22**, 4466–4479 (2014).
160. Moroney N, Bino LD, Woodley MTM, Ghalanos GN, Silver JM et al. Logic gates based on interaction of counterpropagating light in microresonators. *J Lightwave Technol* **38**, 1414–1419 (2020).
161. Wang SH, Li YH, Little BE, Wang LR, Wang X et al. Athermal third harmonic generation in micro-ring resonators. *Opto-Electron Adv* **3**, 200028 (2020).
162. Birr T, Zywietz U, Chhantyal P, Chichkov BN, Reinhardt C. Ultrafast surface plasmon-polariton logic gates and half-adder. *Opt Express* **23**, 31755–31765 (2015).
163. Ota M, Sumimura A, Fukuhara M, Ishii Y, Fukuda M. Plasmonic-multimode-interference-based logic circuit with simple phase adjustment. *Sci Rep* **6**, 24546 (2016).
164. Wu XT, Tian JP, Yang RC. A type of all-optical logic gate based on graphene surface plasmon polaritons. *Opt Commun* **403**, 185–192 (2017).
165. Sharma P, Kumar VD. All optical logic gates using hybrid metal insulator metal plasmonic waveguide. *IEEE Photonics Technol Lett* **30**, 959–962 (2018).
166. Li P, Wang YX, Xu P. All-optical logic gates based on unidirectional surface plasmon polaritons. *Appl Opt* **58**, 4205–4210 (2019).
167. Gogoi N, Sahu PP. All-optical compact surface plasmonic two-mode interference device for optical logic gate operation. *Appl Opt* **54**, 1051–1057 (2015).
168. Ho KS, Han YH, Ri CS, Im SJ. Actively phase-controlled coupling between plasmonic waveguides via in-between gain-assisted nanoresonator: nanoscale optical logic gates. *Opt Lett* **41**, 3739–3742 (2016).
169. Zhu ZB, Yuan J, Jiang LY. Multifunctional and multichannel all-optical logic gates based on the in-plane coherent control of localized surface plasmons. *Opt Lett* **45**, 6362–6365 (2020).
170. Liu Q, Li N, Tan CH. All-optical logic gate based on manipulation of surface polaritons solitons via external gradient magnetic fields. *Phys Rev A* **101**, 023818 (2020).
171. Sang YG, Wu XJ, Raja SS, Wang CY, Li HZ et al. Broadband multifunctional plasmonic logic gates. *Adv Opt Mater* **6**, 1701368 (2018).
172. Lu CC, Hu XY, Yue S, Fu YL, Yang H et al. Ferroelectric hybrid plasmonic waveguide for all-optical logic gate applications. *Plasmonics* **8**, 749–754 (2013).
173. Cohen M, Zalevsky Z, Shavit R. Towards integrated nanoplasmonic logic circuitry. *Nanoscale* **5**, 5442–5449 (2013).
174. Liu HQ, Quan ZQ, Cheng Y, Deng SJ, Yuan LB. Ultra-compact universal linear-optical logic gate based on single rectangle plasmonic slot nanoantenna. *Plasmonics* **16**, 973–980 (2021).
175. Li F, Vo TD, Husko C, Pelusi M, Xu DX et al. All-optical XOR logic gate for 40Gb/s DPSK signals via FWM in a silicon nanowire. *Opt Express* **19**, 20364–20371 (2011).
176. Yin ZS, Wu J, Zang JZ, Kong DM, Qiu JF et al. All-optical logic gate for XOR operation between 40-Gbaud QPSK tributaries in an ultra-short silicon nanowire. *IEEE Photonics J* **6**, 4500307 (2014).
177. Wei H, Li ZP, Tian XR, Wang ZX, Cong FZ et al. Quantum dot-based local field imaging reveals plasmon-based interferometric logic in silver nanowire networks. *Nano Lett* **11**, 471–475 (2011).
178. Wei H, Wang ZX, Tian XR, Käll M, Xu HX. Cascaded logic gates in nanophotonic plasmon networks. *Nat Commun* **2**, 387 (2011).
179. Piccione B, Cho CH, van Vugt LK, Agarwal R. All-optical active switching in individual semiconductor nanowires. *Nat Nanotech* **7**, 640–645 (2012).
180. Gao L, Chen L, Wei H, Xu HX. Lithographically fabricated gold nanowire waveguides for plasmonic routers and logic gates. *Nanoscale* **10**, 11923–11929 (2018).
181. Yang H, Khayrudinov V, Dhaka V, Jiang H, Autere A et al. Nanowire network-based multifunctional all-optical logic gates. *Sci Adv* **4**, eaar7954 (2018).
182. Lv YC, Xu FF, Wang K, Li YJ, Zhao YS. Loss compensation of surface plasmon polaritons in organic/metal nanowire heterostructures toward photonic logic processing. *Sci China Mater* **63**, 1464–1471 (2020).
183. Salmanpour A, Mohammadnejad S, Bahrami A. Photonic crystal logic gates: an overview. *Opt Quant Electron* **47**, 2249–2275 (2015).
184. Caballero LEP, Neto OPV. A review on photonic crystal logic gates. *J Integr Circuits Syst* **16**, 1–13 (2021).
185. Zhang YL, Zhang Y, Li BJ. Optical switches and logic gates based on self-collimated beams in two-dimensional photonic crystals. *Opt Express* **15**, 9287–9292 (2007).
186. Christina XS, Kabilan AP. Design of optical logic gates using self-collimated beams in 2D photonic crystal. *Photonic Sens* **2**, 173–179 (2012).
187. Fan RR, Yang XL, Meng XF, Sun XW. 2D photonic crystal logic gates based on self-collimated effect. *J Phys D Appl Phys* **49**, 325104 (2016).
188. Ishizaka Y, Kawaguchi Y, Saitoh K, Koshiba M. Design of ultra compact all-optical XOR and AND logic gates with low power consumption. *Opt Commun* **284**, 3528–3533 (2011).
189. Liu WJ, Yang DQ, Shen GS, Tian HP, Ji YF. Design of ultra compact all-optical XOR, XNOR, NAND and OR gates using

photonic crystal multi-mode interference waveguides. *Opt Laser Technol* **50**, 55–64 (2013).
190. Tang CR, Dou XY, Lin YX, Yin HX, Wu B et al. Design of all-optical logic gates avoiding external phase shifters in a two-dimensional photonic crystal based on multi-mode interference for BPSK signals. *Opt Commun* **316**, 49–55 (2014).
191. Zhu ZH, Ye WM, Ji JR, Yuan XD, Zen C. High-contrast light-by-light switching and AND gate based on nonlinear photonic crystals. *Opt Express* **14**, 1783–1788 (2006).
192. Fu YL, Hu XY, Gong QH. Silicon photonic crystal all-optical logic gates. *Phys Lett A* **377**, 329–333 (2013).
193. Rani P, Kalra Y, Sinha RK. Realization of AND gate in Y shaped photonic crystal waveguide. *Opt Commun* **298 –299**, 227–231 (2013).
194. Rani P, Kalra Y, Sinha RK. Design of all optical logic gates in photonic crystal waveguides. *Optik* **126**, 950–955 (2015).
195. Singh BR, Rawal S. Photonic-crystal-based all-optical NOT logic gate. *J Opt Soc Am A* **32**, 2260–2263 (2015).
196. Rao DGS, Swarnakar S, Kumar S. Performance analysis of all-optical NAND, NOR, and XNOR logic gates using photonic crystal waveguide for optical computing applications. *Opt Eng* **59**, 057101 (2020).
197. Mohebzadeh-Bahabady A, Olyaee S. All-optical NOT and XOR logic gates using photonic crystal nano-resonator and based on an interference effect. *IET Optoelectron* **12**, 191–195 (2018).
198. Parandin F, Malmir MR, Naseri M, Zahedi A. Reconfigurable all-optical NOT, XOR, and NOR logic gates based on two dimensional photonic crystals. *Superlattices Microstruct* **113**, 737–744 (2018).
199. Goudarzi K, Mir A, Chaharmahali I, Goudarzi D. All-optical XOR and OR logic gates based on line and point defects in 2-D photonic crystal. *Opt Laser Technol* **78**, 139–142 (2016).
200. Lu CH, Zhu B, Zhu CY, Ge LC, Liu Y et al. All-optical logic gates and a half-adder based on lithium niobate photonic crystal micro-cavities. *Chin Opt Lett* **17**, 072301 (2019).
201. Isfahani BM, Tameh TA, Granpayeh N, Javan ARM. All-optical NOR gate based on nonlinear photonic crystal microring resonators. *J Opt Soc Am B* **26**, 1097–1102 (2009).
202. Bai JB, Wang JQ, Jiang JZ, Chen XY, Li H et al. Photonic not and nor gates based on a single compact photonic crystal ring resonator. *Appl Opt* **48**, 6923–6927 (2009).
203. Andalib P, Granpayeh N. All-optical ultra-compact photonic crystal NOR gate based on nonlinear ring resonators. *J Opt A Pure Appl Opt* **11**, 085203 (2009).
204. Andalib P, Granpayeh N. All-optical ultracompact photonic crystal AND gate based on nonlinear ring resonators. *J Opt Soc Am B* **26**, 10–16 (2009).
205. Alipour-Banaei H, Serajmohammadi S, Mehdizadeh F. All optical NOR and NAND gate based on nonlinear photonic crystal ring resonators. *Optik* **125**, 5701–5704 (2014).
206. Pirzadi M, Mir A, Bodaghi D. Realization of ultra-accurate and compact all-optical photonic crystal OR logic gate. *IEEE Photonics Technol Lett* **28**, 2387–2390 (2016).
207. D'souza NM, Mathew V. Interference based square lattice photonic crystal logic gates working with different wavelengths. *Opt Laser Technol* **80**, 214–219 (2016).
208. Moniem TA. All-optical XNOR gate based on 2D photonic-crystal ring resonators. *Quant Electron* **47**, 169–172 (2017).
209. Hussein HME, Ali TA, Rafat NH. New designs of a complete set of Photonic Crystals logic gates. *Opt Commun* **411**, 175–181 (2018).
210. Salimzadeh A, Alipour-Banaei H. An all optical 8 to 3 encoder based on photonic crystal OR-gate ring resonators. *Opt Commun* **410**, 793–798 (2018).
211. Younis RM, Areed NFF, Obayya SSA. Fully integrated AND and OR optical logic gates. *IEEE Photonics Technol Lett* **26**, 1900–1903 (2014).
212. Liu Y, Qin F, Meng ZM, Zhou F, Mao QH et al. All-optical logic gates based on two-dimensional low-refractive-index nonlinear photonic crystal slabs. *Opt Express* **19**, 1945–1953 (2011).
213. Yanik MF, Fan SH, Soljačić M. High-contrast all-optical bistable switching in photonic crystal microcavities. *Appl Phys Lett* **83**, 2739–2741 (2003).
214. Yanik MF, Fan SH, Soljačić M, Joannopoulos JD. All-optical transistor action with bistable switching in a photonic crystal cross-waveguide geometry. *Opt Lett* **28**, 2506–2508 (2003).
215. Vujic D, John S. Pulse reshaping in photonic crystal waveguides and microcavities with Kerr nonlinearity: Critical issues for all-optical switching. *Physical Review A* **72**, 013807 (2005).
216. Nozaki K, Tanabe T, Shinya A, Matsuo S, Sato T et al. Sub-femtojoule all-optical switching using a photonic-crystal nanocavity. *Nat Photonics* **4**, 477–483 (2010).
217. Jandieri V, Khomeriki R, Erni D. Realization of true all-optical AND logic gate based on nonlinear coupled air-hole type photonic crystal waveguides. *Opt Express* **26**, 19845–19853 (2018).
218. Jandieri V, Khomeriki R, Onoprishvili T, Werner DH, Berakdar J et al. Functional all-optical logic gates for true time-domain signal processing in nonlinear photonic crystal waveguides. *Opt Express* **28**, 18317–18331 (2020).
219. Caballero LP, Povinelli ML, Ramirez JC, Guimarães PSS, Neto OPV. Complementary photonic crystal integrated logic devices. *Opt Lett* **45**, 5502–5505 (2020).
220. He L, Zhang WX, Zhang XD. Topological all-optical logic gates based on two-dimensional photonic crystals. *Opt Express* **27**, 25841–25859 (2019).
221. He L, Ji HY, Wang YJ, Zhang XD. Topologically protected beam splitters and logic gates based on two-dimensional silicon photonic crystal slabs. *Opt Express* **28**, 34015–34023 (2020).
222. Coelho AG, Costa MBC, Ferreira AC, da Silva MG, Lyra ML et al. Realization of all-optical logic gates in a triangular triple-core photonic crystal fiber. *J Lightwave Technol* **31**, 731–739 (2013).
223. Sousa JRR, Filho AFGF, Ferreira AC, Batista GS, Sobrinho CS et al. Generation of logic gates based on a photonic crystal fiber Michelson interferometer. *Opt Commun* **322**, 143–149 (2014).
224. Kumar S, Sen M. Integrable all-optical NOT gate using nonlinear photonic crystal MZI for photonic integrated circuit. *J Opt Soc Am B* **37**, 359–369 (2020).
225. Datta T, Sen M. Raman mediated ultrafast all-optical nor gate. *Appl Opt* **59**, 6352–6359 (2020).
226. Dhasarathan V, Sahu SK, Nguyen TK, Palai G. Realization of all logic gates using metamaterials based three dimensional photonics structures: a future application of 3D photonics to optical computing. *Optik* **202**, 163723 (2020).
227. Ginzburg P, Orenstein M. Photonic switching in waveguides using spatial concepts inspired by EIT. *Opt Express* **14**,

11312–11317 (2006).
228. Ginzburg P, Hayat A, Vishnyakov V, Orenstein M. Photonic logic by linear unidirectional interference. *Opt Express* **17**, 4251–4256 (2009).
229. Raghuwanshi SK, Kumar A, Kumar S. 1 × 4 signal router using three Mach-Zehnder interferometers. *Opt Eng* **52**, 035002 (2013).
230. Tang XF, Fang ZQ, Zhai YX, Jiao XS, Gao N et al. A reconfigurable optical logic gate with up to 25 logic functions based on polarization modulation with direct detection. *IEEE Photonics J* **9**, 7802011 (2017).
231. Ooi KJA, Chu HS, Bai P, Ang LK. Electro-optical graphene plasmonic logic gates. *Opt Lett* **39**, 1629–1632 (2014).
232. Ying ZF, Soref R. Electro-optical logic using dual-nanobeam Mach-Zehnder interferometer switches. *Opt Express* **29**, 12801–12812 (2021).
233. Min SC, Liao SS, Zou CL, Zhang XL, Dong JJ. Route-asymmetrical optical transmission and logic gate based on optical gradient force. *Opt Express* **22**, 25947–25952 (2014).
234. Zhang YH, Xiang SY, Cao XY, Zhao SH, Guo XX et al. Experimental demonstration of pyramidal neuron-like dynamics dominated by dendritic action potentials based on a VCSEL for all-optical XOR classification task. *Photonics Res* **9**, 1055–1061 (2021).
235. Xiang SY, Ren ZX, Zhang YH, Song ZW, Hao Y. All-optical neuromorphic XOR operation with inhibitory dynamics of a single photonic spiking neuron based on a VCSEL-SA. *Opt Lett* **45**, 1104–1107 (2020).
236. Wu LM, Fan TJ, Wei SR, Xu YJ, Zhang Y et al. All-optical logic devices based on black arsenic–phosphorus with strong nonlinear optical response and high stability. *Opto-Electron Adv* **5**, 200046 (2022).
237. Miller DAB. Are optical transistors the logical next step. *Nat Photonics* **4**, 3–5 (2010).
238. Qiu CY, Xiao HF, Wang LH, Tian YH. Recent advances in integrated optical directed logic operations for high performance optical computing: a review. *Front Optoelectron* **15**, 1 (2022).
239. Ying ZF, Feng CH, Zhao Z, Dhar S, Dalir H et al. Electronic-photonic arithmetic logic unit for high-speed computing. *Nat Commun* **11**, 2154 (2020).
240. Boolakee T, Heide C, Garzón-Ramírez A, Weber HB, Franco I et al. Light-field control of real and virtual charge carriers. *Nature* **605**, 251–255 (2022).
241. Lei L, Dong JJ, Yu Y, Tan SS, Zhang XL. All-optical canonical logic units-based programmable logic array (CLUs-PLA) using semiconductor optical amplifiers. *J Lightwave Technol* **30**, 3532–3539 (2012).
242. Caballero LP, Povinelli ML, Ramirez JC, Guimarães PSS, Neto OPV. Photonic crystal integrated logic gates and circuits. *Opt Express* **30**, 1976–1993 (2022).
243. Chen XB, Yu Y, Zhang XL. All-optical logic minterms for three-input demodulated differential phase-shift keying signals at 40Gb/s. *IEEE Photonics Technol Lett* **23**, 118–120 (2011).
244. Reis C, Maziotis A, Kouloumentas C, Stamatiadis C, Bougioukos M et al. All-optical synchronous S-R flip-flop based on active interferometric devices. *Electron Lett* **46**, 709–710 (2010).
245. Aikawa Y, Shimizu S, Uenohara H. Demonstration of all-optical divider circuit using SOA-MZI-type XOR gate and feedback loop for forward error detection. *J Lightwave Technol* **29**, 2259–2366 (2011).
246. Wang Y, Zhang XL, Dong JJ, Huang DX. Simultaneous demonstration on all-optical digital encoder and comparator at 40 Gb/s with semiconductor optical amplifiers. *Opt Express* **15**, 15080–15085 (2007).
247. Lin X, Liu JP, Hao JY, Wang K, Zhang YY et al. Collinear holographic data storage technologies. *Opto-Electron Adv* **3**, 190004 (2020).
248. Hardy J, Shamir J. Optics inspired logic architecture. *Opt Express* **15**, 150–165 (2007).
249. Wang YH, He S, Gao XY, Ye PP, Lei L et al. Enhanced optical nonlinearity in a silicon–organic hybrid slot waveguide for all-optical signal processing. *Photonics Res* **10**, 50–58 (2022).
250. Wang C, Li F, Xu Y, Duan M, Song Y et al. Tin Selenide: a promising black-phosphorus-analogue nonlinear optical material and its application as all-optical switcher and all-optical logic gate. *Mater Today Phys* **21**, 100500 (2021).

Acknowledgements

This work is partially supported by the National Key Research and Development Program of China (Grants No.2021YFA1401500), the National Natural Science Foundation of China (12022416), the Department of Natural Resources of Guangdong Province (No. GDNRC[2022] 22), Department of Science and Technology of Guangdong Province (No. 2021A0505080002), Intelligent Laser Basic Research Laboratory (No. PCL2021A14-B1), and the Hong Kong Research Grants Council (16306220).

Competing interests

The authors declare no competing financial interests.